Accepted Manuscript

Variant-dependent heterogeneity in amyloid β burden in autosomal dominant Alzheimer's disease: cross-sectional and longitudinal analyses of an observational study

Jasmeer P Chhatwal MD, Stephanie A Schultz PhD, Eric McDade DO, Aaron P Schultz PhD, Lei Liu MD, Bernard J Hanseeuw MD, Nelly Joseph-Mathurin PhD, Rebecca Feldman BS, Colleen D Fitzpatrick BS, Kathryn P Sparks BA, Johannes Levin Prof, Sarah B Berman MD, Alan E Renton PhD, Bianca T Esposito BS, Maria Vitoria Fernandez PhD, Yun Ju Sung PhD, Jae Hong Lee Prof, William E Klunk Prof, Anna Hofmann MD, James M Noble MD, Neill Graff-Radford Prof, Hiroshi Mori Prof, Steven M Salloway Prof, Colin L Masters Prof, Ralph Martins Prof, Celeste M Karch PhD, Chengjie Xiong Prof, Carlos Cruchaga Prof, Richard J Perrin MD, Brian A Gordon PhD, Tammie L S Benzinger Prof, Nick C Fox Prof, Peter R Schofield Prof, Anne M Fagan Prof, Alison M Goate Prof, John C Morris Prof, Randall J Bateman Prof, Keith A Johnson Prof, Reisa A Sperling Prof

PII: S1474-4422(21)00375-6
DOI: doi:10.1016/S1474-4422(21)00375-6
Reference: LANEUR 2073

Published in: *The Lancet Neurology*

Cite this article as: Chhatwal JP, Schultz SA, McDade E, Schultz AP, Liu L, Hanseeuw BJ, Joseph-Mathurin N, Feldman R, Fitzpatrick CD, Sparks KP, Levin J, Berman SB, Renton AE, Esposito BT, Fernandez MV, Sung YJ, Lee JH, Klunk WE, Hofmann A, Noble JM, Graff-Radford N, Mori H, Salloway SM, Masters CL, Martins R, Karch CM, Xiong C, Cruchaga C, Perrin RJ, Gordon BA, Benzinger TLS, Fox NC, Schofield PR, Fagan AM, Goate AM, Morris JC, Bateman RJ, Johnson KA, Sperling RA, Variant-dependent heterogeneity in amyloid β burden in autosomal dominant Alzheimer's disease: cross-sectional and longitudinal analyses of an observational study, ***The Lancet Neurology***, doi:10.1016/S1474-4422(21)00375-6

Title**: Assessing Variant-Dependent Heterogeneity in β-Amyloid Burden in Autosomal Dominant Alzheimer's Disease: a cross-sectional and longitudinal study**

Jasmeer P Chhatwal, MD, Stephanie A Schultz, PhD, Eric McDade, DO, Aaron P Schultz, PhD, Lei Liu, MD, Bernard J Hanseeuw, MD, Nelly Joseph-Mathurin, PhD, Rebecca Feldman, BS, Colleen D Fitzpatrick, BS, Kathryn P Sparks, BA, Prof Johannes Levin, MD, Sarah B Berman, MD, Alan E Renton, PhD, Bianca T Esposito, BS, Maria Vitoria Fernandez, PhD, Yun Ju Sung, PhD, Prof Jae Hong Lee, MD, Prof William E Klunk, MD, Anna Hofmann, MD, James M Noble, MD, Prof Neill Graff-Radford, MD, Prof Hiroshi Mori, PhD, Prof Steven M Salloway, MD, Prof Colin L Masters, MD, Prof Ralph Martins, PhD, Celeste M Karch, PhD, Prof Chengjie Xiong, PhD, Prof Carlos Cruchaga, PhD, Richard J Perrin, MD, Brian A Gordon, PhD, Prof Tammie LS Benzinger, MD, Prof Nick C Fox, MD, Prof Peter R Schofield, PhD, Prof Anne M Fagan, PhD, Prof Alison M Goate, DPhil, Prof John C Morris, MD, Prof Randall J Bateman, MD, Prof Keith A Johnson, MD, Prof Reisa A Sperling, MD, for the Dominantly Inherited Alzheimer's Network Investigators

Keywords: amyloid, genotype, Presenilin, Amyloid Precursor Protein, Alzheimer's Disease

Background:
Examination of autosomal dominant Alzheimer's disease has broadly influenced mechanistic hypotheses, biomarker development, and clinical trials in both sporadic and dominantly-inherited Alzheimer's disease. While pathogenic variants causing autosomal dominant Alzheimer's disease are highly-penetrant, there is substantial heterogeneity in β-amyloid levels across individuals. We examined whether this heterogeneity is related to disease progression and its association with mutation location within *PSEN1, PSEN2, or APP*.

Methods:
We examined variant-dependent variability in Pittsburgh-Compound-B PET (PiB-PET) signal, CSF Aβ42 and Aβ40 in 347 participants (206 carriers) in the Dominantly Inherited Alzheimer's Network Observational Study assessed from 2008 to 2019. Two approaches were used to group the 62 unique pathogenic variants in the cohort: (1) based on affected protein domain in PSEN1, PSEN2, or APP, and (2) based on whether *PSEN1* variants were before or after codon 200.

Findings:
Cortical and striatal PiB-PET signal demonstrated striking variant-dependent variability using both grouping approaches, despite similar progression on the Clinical Dementia Rating and CSF Aβ42 levels. Longitudinal PiB-PET signal also varied across codon-based groups, mirroring cross-sectional analyses.

Interpretation:
Autosomal dominant Alzheimer's disease pathogenic variants demonstrated highly differential temporal and regional patterns of β-amyloid PET, despite similar functional progression. This suggests that while increased β-amyloid PET signal is generally seen

in autosomal dominant Alzheimer's disease, higher levels of β-amyloid PET signal at an individual level may not reflect more severe or more advanced disease – an important consideration for ongoing clinical trials, including those using β-amyloid PET as a surrogate measure of disease progression. Also germane to both sporadic and autosomal dominant Alzheimer's disease, the results here suggest CSF and PET measures of β-amyloid levels are not interchangeable and may reflect different amyloid-driven pathobiological processes.

Funding: National Institute on Aging (UF1AG032438;R01AG036694;K23049087), Doris Duke Charitable Foundation, German Center for Neurodegenerative Diseases, and Japanese Agency for Medical Research and Development.

Department of Neurology, Harvard Medical School, Boston, MA, USA (JPC, SAS, APS, BJH, LL, KAJ, RAS)
Massachusetts General Hospital, Boston, MA, USA (JPC, SAS, APS, BJH, CF, KPS, KAJ, RAS)
Brigham and Women's Hospital, Boston, MA, USA (JPC, LL, CF, KAJ, RAS)
Department of Neurology, Washington University in St. Louis, St. Louis, MO, USA (EM, CMK, AMF, JCM, RJB)
Université Catholique de Louvain, Brussels B-1348, Belgium (BJH)
Mallinckrodt Institute of Radiology, Washington University in St. Louis, St. Louis, MO, USA (NJM, RF, BAG, TLSB)
German Center for Neurodegenerative Diseases (DZNE) Munich, Germany (JL)
Department of Neurology, Ludwig-Maximilians Universität München, Munich, Germany (JL)
Munich Cluster for Systems Neurology (SyNergy), Munich, Germany (JL)
Department of Neurology, University of Pittsburgh, Pittsburgh, PA, USA (SBB, WEK)
German Center for Neurodegenerative Disease, Tübingen, Germany (AH)
Department of Neurology, Asan Medical Center, University of Ulsan College of Medicine, Seoul, Korea (JHL)
Department of Psychiatry, University of Pittsburgh, Pittsburgh, PA, USA (WEK)
Columbia University Irving Medical Center, Department of Neurology, New York, NY, USA (JMN)
Mayo Clinic, Department of Neurology, Jacksonville, FL, USA (NGR)
Osaka City University, Sumiyoshi Ward, Osaka, Japan (HM)
UCL Queen Square Institute of Neurology, Dementia Research Centre, London WC1 3BG, United Kingdom (NF)
Butler Hospital, Memory and Aging Program, Brown University Alpert Medical School, Providence, RI, USA (SMS)
The University of Melbourne, Melbourne, Victoria, Australia (CLM)
Florey Institute, Melbourne, Victoria, Australia (CLM)
Department of Psychiatry, Washington University in St. Louis School of Medicine, St. Louis, MO, USA (CC, MVF, YJS)
Division of Biostatistics, Washington University in St. Louis School of Medicine, St. Louis, MO, USA (CX)

Department of Biomedical Sciences, Macquarie University, Sydney, NSW, Australia (RM)
Department of Pathology, Washington University in St. Louis School of Medicine, St. Louis, MO, USA (RP)
Neuroscience Research Australia, Sydney, NSW, Australia (PRS)
School of Medical Sciences, University of South Wales, Sydney NSW, Australia (PRS)
Department of Neuroscience, Icahn School of Medicine at Mount Sinai, New York, NY (AER, BTE, AMG)

Research in Context:

Evidence before this study: All relevant articles on PubMed relating to autosomal dominant Alzheimer's disease pathogenic variants affecting β-amyloid burden (both assessed with PET and cerebrospinal fluid; CSF) were regularly searched from October 2018 to May 2021 and considered for inclusion in the present report. Search terms included: dominantly inherited Alzheimer's disease, autosomal dominant Alzheimer's disease, amyloid PET, *PSEN1*, *PSEN2*, *APP*, CSF, Aβ42, and Aβ40. Previous studies, particularly those from the Dominantly Inherited Alzheimer's Network (DIAN) and the Alzheimer's Prevention Initiative have characterized the behavior of CSF Aβ42 and β-amyloid PET across a wide spectrum of asymptomatic and symptomatic autosomal dominant Alzheimer's disease. Due to limited diversity of autosomal dominant Alzheimer's disease genotypes and sample size, these studies either did not examine the role of individual pathogenic variants or used broad genotype categories (e.g., *PSEN1* pre- and post-codon 200, all *PSEN1* compared to all *APP* pathogenic variant carriers) in relatively small samples.

Added value of the study: The study of autosomal dominant Alzheimer's disease offers a unique and powerful venue to critically assess Alzheimer's disease biomarkers and their relationships to disease progression. Combining autosomal dominant Alzheimer's disease pathogenic variant carriers into broad groups (carriers vs. non-carriers; *PSEN1* carriers vs. *APP* carriers, etc.) makes it difficult to recognize the heterogeneity in amyloid burden between variants and determine the extent to which variations in amyloid burden are mirrored by variations in disease progression. We leverage the unique size and diversity of pathogenic variants present in the DIAN cohort to assess variant-dependent variability in amyloid burden and disease progression in a way that has not previously been possible. The relationship of PET and CSF amyloid measures to each other and to disease progression may have important implications for the execution of ongoing clinical trials in both sporadic and dominantly-inherited Alzheimer's disease. This is particularly the case for the use of amyloid PET as a surrogate efficacy marker and proxy for disease stage in ongoing clinical trials. More broadly, the presence of heterogeneity in amyloid measures in autosomal dominant Alzheimer's disease may have mechanistic implications for understanding how pathologic amyloid-driven processes promote disease progression in Alzheimer's disease and the extent to which commonly used Alzheimer's disease biomarkers accurately reflect these pathologic processes.

Implications of all of the available evidence: Prior work in which *PSEN1* pathogenic variant carriers were categorized by whether their variant was before or after codon 200 suggests that post-codon 200 variant carriers were more likely to have cerebral amyloid angiopathy, whereas those with variants pre-codon 200 had shorter disease duration. However, the data presented here in a comparatively large and genetically diverse sample suggest that disease progression is very similar in carriers of pre- and post-codon 200 *PSEN1* variants, despite the overall higher levels of PiB PET signal in pre-codon 200 carriers. Consistent with cross-sectional findings in pre- and post-codon 200 *PSEN1* carriers, longitudinal data demonstrate higher rates β-amyloid PET signal increase in pre-codon 200 carriers, particularly during the symptomatic phase of disease. While prior studies in small and less genetically-diverse samples suggest that striatal β-amyloid accumulation may precede cortical β-amyloid deposition, the present results strongly suggest that this striatal predominant pattern is not universal across autosomal dominant Alzheimer's disease and may be present in only a subset of *PSEN1* pathogenic variants. For many variant groupings, striatal and cortical PiB PET signal rose in tandem. Additionally, cortical predominant patterns were also observed. Relevant to both sporadic Alzheimer's disease and autosomal dominant Alzheimer's disease, the observed discordance in some variants between CSF and PET measures of β-amyloid burden raises questions regarding how interchangeable these measures are in assessing an individual's disease stage and potential response to therapy in a clinical trial. As variations in β-amyloid were not tightly associated with variations functional progression, these results may have broader implications for understanding how closely these widely used amyloid biomarkers mirror amyloid-related pathogenic processes and the extent to which these β-amyloid biomarkers can be considered surrogate markers of disease progression at an individual level.

Introduction:

Biomarkers play an increasingly critical role in Alzheimer's disease therapeutic development, as demonstrated by the recent accelerated approval of the anti-amyloid monocolonal antibody Aduhelm (aducanumab-avwa) based on reductions in β-amyloid PET signal. Cases of autosomal dominant Alzheimer's disease have been central to the development of Alzheimer's disease biomarkers, forming the basis for many animal models of Alzheimer's disease, and offering strong support for the β-amyloid hypothesis of Alzheimer's disease. The nearly complete penetrance and conserved age of symptom onset within families (though with some variability[1]) also allows for an understanding of where an autosomal dominant Alzheimer's disease carrier may be in the overall disease course even in asymptomatic phases of disease. In turn, this offers a rare opportunity to critically examine the temporal course of Alzheimer's disease biomarker changes that culminate in symptom onset and to identify biomarkers that are most closely tied to cognitive and functional impairment.

More than 300 highly penetrant, pathogenic variants in *PSEN1*, *PSEN2*, and *APP* leading to autosomal dominant forms of Alzheimer's Disease have been identified, clearly implicating Aβ production and processing as central to Alzheimer's disease pathobiology[2,3]. Autosomal dominant Alzheimer's disease causing genetic variants are believed to drive disease by altering the relative amounts of Aβ peptides generated through the processing of APP[4], such that longer, more aggregation prone Aβ species (especially Aβ42 and Aβ43) increase in abundance relative to shorter, less aggregation-prone Aβ fragments[5,6], thereby increasing deposition of fibrillar β-amyloid in extracellular plaques[7]. However, there is substantial biochemical evidence demonstrating variability in the Aβ peptide profiles produced by different autosomal dominant Alzheimer's disease-causing variants, despite their nearly complete penetrance[8,9]. In turn, this variability in Aβ production and other genotype-dependent changes in γ-secretase function[10-12] may alter the observed biomarker trajectories across variants. In the present report we examine the variability in β-amyloid burden across autosomal dominant Alzheimer's disease pathogenic variants, allowing us to identify variant-specific effects on biomarker trajectories and assess how these variations may be associated with variations in functional decline.

The Dominantly Inherited Alzheimer's Network (DIAN) is an international, multi-site observational study that enrolls individuals from families harboring autosomal dominant Alzheimer's disease pathogenic variants[2]. DIAN has gathered data from over 100 families bearing more than 60 unique pathogenic variants leading to autosomal dominant Alzheimer's disease. The diversity of variants found in the DIAN cohort offers an opportunity to assess whether variations in biomarker trajectories are present across pathogenic variants. Here we leverage this opportunity to examine variant-dependent variability in CSF and PET measures of β-amyloid. The impact of pathogenic variants on β-amyloid burden as measured by PIB PET and CSF β-amyloid across pre-symptomatic and symptomatic disease has important implications for the evaluation of Alzheimer's

disease therapeutics, both in autosomal dominant and sporadic, late-onset Alzheimer's disease. Given the relative certainty that pathogenic variant carriers are on an Alzheimer's disease trajectory, heterogeneity in β-amyloid PET and CSF measures can broadly inform understanding of how precisely these biomarkers reflect amyloid-driven processes that underlie the progression of Alzheimer's disease at an individual level.

Methods:

Participants

Data from 347 participants (206 pathogenic variant carriers, 141 non-carriers, 112 families) in the DIAN Observational Study recruited between September 2008 and June 2019 were included. Participants provided informed consent in accordance with the local institutional review boards of each participating site. Each participant's estimated years from symptom onset (EYO) was calculated as the participant's age minus the age at which the participant's family member(s) first showed symptoms of progressive cognitive decline. Negative values for EYO indicate that the participant is younger than their familial age of symptom onset and positive values indicate that a participant is older than their familial age of onset. Clinical dementia rating (CDR) global and sum-of-boxes (SOB) scores were measured for each participant at each visit using structured interviews, as previously described[2]. All participants[2,13] bearing pathogenic variants (see supplemental methods) and with available genetic, clinical, imaging, and CSF data were included.

Genotyping:

The presence of autosomal dominant Alzheimer's disease pathogenic variants (Sanger sequencing) and APOE genotype (PCR-based) were assessed using DNA derived in parallel at the DIAN Genetics Core (Mount Sinai School of Medicine) and the National Cell Repository for Alzheimer's Disease (NCRAD), as previously described[2].

Variant Grouping:

To facilitate assessment of pathogenic variant-dependent variability in β-amyloid burden, the 62 unique autosomal dominant Alzheimer's disease variants present in the cohort were grouped using two approaches (Figure 1A-D). Individuals were first grouped by the affected protein domain in PSEN1, PSEN2 or APP impacted by the underlying autosomal dominant Alzheimer's disease-causing variant, using annotation available in UniProt. Domain-based groupings with greater than 10 pathogenic variant carriers were retained as distinct groups for the purposes of statistical modeling, resulting in 9 retained domain-based groups. (Figure 1D). Each domain-based grouping represented at least 2 families, and all but one represented more than one pathogenic variant (Supplemental Tables 1 and 2). Note that the APP Transmembrane Domain grouping is comprised of variants at or near the γ-secretase cleavage site (Figure 1C). The small number (n=4) of remaining APP pathogenic variant carriers (including those with variants near the β-secretase cleavage site) were not retained as a distinct group, but were included with the Ungrouped pathogenic variant carriers (Figure 1D).

In the second approach, only individuals with pathogenic variants in *PSEN1* were included and were grouped based on whether the underlying variant is before or after codon 200 in *PSEN1*[14,15]. Codon 200 falls within PSEN1 transmembrane domain 4, but all carriers with transmembrane domain 4 variants in the cohort are post-codon 200 (Figure 1A). Consequently, PSEN1 transmembrane 1-3, cytoplasmic 1-2, and luminal 1-2 domain carriers are included in the prior-to-codon 200 grouping, and all remaining PSEN1 carriers are included in the post-codon 200 grouping (Figure 1; Supplemental Table 1).

Procedures:

11-C-Pittsburgh Compound-B (PiB PET) was performed as previously described [2,13]. Binding was assessed 40–70 min following PiB bolus and converted to cortical gray matter and dorsal striatal (averaging bilateral caudate and putamen) mean standardized uptake value ratios (SUVRs) using cerebellar gray matter as the reference region and employing regional spread function based partial volume correction. Sensitivity analyses using FreeSurfer-defined cortical white matter or brainstem as reference regions demonstrated that the effects reported are not reference region dependent (Supplemental Table 3).

Cerebrospinal fluid (CSF) was obtained as previously described using procedures consistent with Alzheimer's Disease Neuroimaging Initiative. CSF analyses for Aβ1-40 (Aβ40) and Aβ1-42 (Aβ42) were performed at the DIAN Biomarker Core using enzyme-linked immunosorbant assay (INNOTEST, Innogenetics, Ghent, Belgium).

Statistical analysis:

General linear mixed effects models were implemented in R (v4.0.0, R Foundation for statistical computing) using the nlme, lmer, parameters, and influence.ME packages. Satterthwaite approximations were used to calculate degrees of freedom. P-values shown are False Discovery Rate (FDR) adjusted. Domain- or codon-based variant group was interacted with EYO to assess variant dependent effects across the disease course. Cross-sectional analyses included age, gender, and binarized *APOE* ε4 status (ε4 carrier or non-carrier) as fixed effects and family membership as a random effect. Models using longitudinal data included the same covariates as cross-sectional models, and further included terms for a random intercept and slope. A variant grouping by time interaction was included as a fixed effect to assess variant-dependent effects on biomarker trajectories in models using longitudinal data. Locally weighted estimated scatter plot smoothing (LOESS) was used for illustrations. Sensitivity analyses assessing family membership, APOE ε4 or ε2 genotype, and Alzheimer's disease polygenic risk scores are described in supplemental methods.

Role of Funding Agencies:

The funders had no direct role in data collection, analysis, interpretation of findings, writing of the manuscript, or decision to submit for publication.

Results:

We first examined relationships between proximity to symptom onset (estimated years to symptom onset; EYO) and β-amyloid burden using both PET and CSF measures. Autosomal dominant Alzheimer's disease pathogenic variant carriers showed significantly lower CSF Aβ42 and higher PiB PET with increasing EYO as compared to non-carriers (CSF Aβ42: β = -16.47 pg/ml/yr (-22.35 to -10.58 95%CI), $p<0.0001$; PiB PET: β = 0.06 SUVR/yr (0.04 to 0.08 95%CI), $p<0.0001$). The decrease in CSF Aβ42 is consistent with prior literature in both sporadic and autosomal dominant Alzheimer's disease[2].

Assessing Variant-Dependent Effects on Functional Progression:

We next assessed whether functional progression of disease varied across variants in autosomal dominant Alzheimer's disease. Mean EYO at study entry was similar across variant groupings (domain: $F(9,196) = 0.67$, $p = 0.75$; codon: $F(1,159) = 0.18$, $p = 0.71$), suggesting that variant groups were statistically similar in terms of proximity to estimated symptom onset. Progression of functional decline as assessed using Clinical Dementia Rating (CDR) sum-of-boxes (SOB) was also similar across variant groupings (domain-based: $F(9,206) = 0.79$, $p = 0.68$; codon-based: $F(1,161) = 0.14$, $p = 0.74$), suggesting similar progression of functional impairment across variant groupings (Figure 3C, F).

Variant Dependent Variations in β-Amyloid Burden Assessed by PiB PET:

We next examined whether β-amyloid burden as measured by PiB-PET varied across variant groupings during autosomal dominant Alzheimer's disease. Significant variant-dependent variability in the relationship between cortical β-amyloid burden and EYO was observed using the domain-based grouping in autosomal dominant Alzheimer's disease pathogenic variant carriers (variant- grouping by EYO interaction: $F(9,170.96) = 5.83$, $p<0.0001$; Figures 3A and 4). Examining this effect more closely, those carrying variants affecting PSEN1 cytoplasmic domain 4 (Grouping by EYO interaction: $F(1, 172.18) = 4.24$, $p = 0.031$; β = -0.045±0.020SE PiB SUVR/yr), PSEN1 transmembrane domain 6 ($F(1,160.18) = 3.98$, $p = 0.047$; β = -0.028±0.014SE PiB SUVR/yr), and PSEN1 transmembrane domain 8 ($F(1, 126.78) = 14.63$, $p = p<0.0001$; β = -0.053±0.014SE PiB SUVR/yr) had less cortical PiB binding in relation to EYO compared to other pathogenic variant carriers. In contrast, PSEN1 transmembrane domain 3 ($F(1, 156.49) = 4.24$, $p = 0.05$; β = 0.089± 0.043SE PiB SUVR/yr), PSEN1 transmembrane 5 ($F(1,198.61) = 5.78$, $p = 0.025$; β = 0.071± 0.029SE PiB SUVR/yr), and PSEN2 transmembrane domain 2 ($F(1, 98.85) = 8.67$, $p<0.0001$; β = 0.050± 0.017SE PiB SUVR/yr) carriers had significantly greater cortical β-amyloid burden in relation to EYO as compared to other pathogenic variant carriers (Figures 3 and 4, Supplemental Figure 2).

Using the *PSEN1* codon-based grouping, we again observed a significant effect of variant grouping on PiB binding relative to EYO, such that those who carried pathogenic variants in *PSEN1* prior to codon 200 had significantly greater cortical PiB PET signal with increasing EYO as compared to those with variants after *PSEN1* codon 200 (codon

category by EYO interaction: $F(1, 154.99) = 21.70$, $p<0.0001$; $\beta = 0.065 \pm 0.014$SE PiB SUVR/yr; Figure 3D). Using a brainstem or white matter reference region instead of cerebellar gray matter yielded similar results for both grouping approaches (Supplemental Table 3), suggesting that variant grouping associations with PiB PET are not reference region dependent.

We next assessed whether similar variant-dependent differences were present in longitudinal PiB PET. Consistent with cross-sectional findings, carriers of *PSEN1* pathogenic variants prior to codon 200 had greater longitudinal rates of PiB PET SUVR increase as compared to carriers of PSEN1 pathogenic variants after codon 200 (n = 77 carriers with 187 observations; codon categorization*time: $t(48.44) = 4.06$, $p<0.0001$; Figure 5C). As clinical trials in autosomal dominant Alzheimer's disease often select participants by EYO range and the presence/absence of symptoms, we repeated these analyses by examining rates of PiB-PET change categorized by these parameters (Figure 5B). We observed that the rates of PiB change were similar across codon-based groupings in early, asymptomatic phases of autosomal dominant Alzheimer's disease, but that significant variant-dependent variability in Aβ burden was evident in later phases of disease (Figure 5). A similar analysis was not performed in the domain-based grouping due to insufficient longitudinal data to model all variant groups across the early, late, and symptomatic phases of disease.

Regional Variations in β-Amyloid Burden:

As prior reports have suggested that the dorsal striatum may be an early and preferential site for β-amyloid deposition in individuals carrying pathogenic variants in *PSEN1*[16-18], we next examined whether variant-based groupings may explain regional variations in striatal vs. cortical β-amyloid burden in pathogenic variant carriers. The relationship between EYO and striatal PiB PET SUVR varied significantly by domain-based grouping ($F(9,167.33) = 2.30$, $p = 0.030$), as did the relative amounts of cortical and striatal PiB PET signal ($F(9,296.02) = 3.87$, $p = 0.0003$; Figure 6A and 6C-K). For most domain-based variant groupings, cortical and striatal PiB PET signal relative were similar in magnitude. However, striatal or cortical predominant patterns were observed in some variant groups. Specifically, the PSEN1 transmembrane domain 4 ($t(296.02) = -2.09$, $p = 0.048$; Figure 6G) and PSEN2 transmembrane 2 ($t(296.02) = -2.726$, $p = 0.010$; Figure 4D and 6K) groupings were observed to have significantly greater cortical vs. striatal β-amyloid burden, whereas the PSEN1 transmembrane 2 ($t(296.02) = 2.44$, $p = 0.033$; Figure 4C, 6E, and Supplemental Figure 3C) and PSEN1 transmembrane domain 8 ($t(296.02) = 2.16$, $p = 0.042$; Figure 4G, 6J) groupings showed greater striatal compared to cortical PiB PET signal. Mirroring the pattern seen with cortical PiB PET signal, *PSEN1* carriers with pathogenic variants prior to codon 200 also had greater striatal PiB PET signal than those with pathogenic variants after codon 200 ($t(159.5) = 3.92$, $p = 0.0003$; Figure 6B).

CSF Measures of β-Amyloid Burden:

We next examined CSF Aβ42 and 40 using the same variant groupings and approach. Unlike the pattern observed with β-amyloid PET, CSF Aβ42 (Figure 2B,D; Supplemental Figure 1) did not show variant dependent variability with respect to EYO using either the domain-based ($F(9,151.86) = 1.77$, $p = 0.095$; Figure 3B) or codon-based groupings ($F(1,160.94) = 0.63$, $p = 0.49$; Figure 3E). The relationship of CSF Aβ42 to PiB PET varied significantly across variants using the domain-based ($F(9, 184.35) = 4.85$, $p = p<0.0001$) but not the *PSEN1* codon 200-based grouping ($F(1,154.99) = 0.4059$, $p = 0.59$). This indicates that that correlations between PET and CSF measures of β-amyloid vary by the PSEN1, 2, or APP protein domain affected by the underlying pathogenic variant (Supplemental Figure 5).

As the CSF Aβ42/40 ratio is commonly used as a means of understanding the relative amounts of aggregation prone Aβ species being produced[5,8], we next examined whether variant-dependent variations in CSF Aβ42/40 were present. Across all autosomal dominant Alzheimer's disease pathogenic variant carriers, Aβ42/40 ratios declined with increasing EYO (effect of increasing EYO in carriers: $t(198.87) = -2.47$, $p = 0.010$). A statistical difference in the CSF Aβ42/40 ratio was seen across variants using the domain-based grouping ($F(9,162.21) = 4.34$, $p<0.0001$) and the *PSEN1* codon 200-based grouping ($F(1,143.39) = 4.9243$, $p = 0.037$). However, including the CSF Aβ42/40 ratio as a covariate did not reduce the effect of variant grouping on PiB-PET SUVR relative to EYO (including CSF Aβ42/40 as a covariate: domain grouping-by-EYO interaction: $F(9,167.74) = 6.138$, $p<0.0001$; codon grouping-by-EYO interaction: $F(1,154.06) = 19.63$, $p<0.0001$; Supplemental Figures 4 and 6). Together, these results indicate that though the CSF Aβ42/40 ratio differs across variant groupings, these differences do not account for the previously observed variant-dependent effects on β-amyloid PET.

Discussion:

Given the central importance of PET and CSF measures of β-amyloid burden to Alzheimer's disease therapeutic development and mechanistic understanding, we used the diversity of autosomal dominant Alzheimer's disease pathogenic variants available in the DIAN observational study to examine whether PET and CSF measures of β-amyloid vary by the underlying pathogenic variant and the extent to which differences in amyloid burden were associated with differences in disease progression. We observed that β-amyloid accumulation as measured by PiB-PET was highly variable across pathogenic variants grouped by the affected protein domain or by the location of the pathogenic variant in *PSEN1*[14]. However, despite robust associations between variant grouping and β-amyloid PET changes with respect to EYO, functional decline was similar across variant groupings. In turn, the results here suggest that β-amyloid PET alone may not represent an optimal surrogate marker of disease stage or severity in autosomal dominant Alzheimer's disease, and that consideration of additional biomarkers, especially measures of soluble Aβ, may be needed in ongoing clinical trials. This includes consideration of blood-based measures of Aβ42/40, which have been recently shown to be highly correlated with cognitive benefit or decline in recent clinical trials of the anti-amyloid agent lecanemab and have also been associated with variations in β-amyloid PET signal

in autosomal dominant Alzheimer's disease[19,20]. Relevant to both sporadic and autosomal dominant Alzheimer's disease, the observed variability between PET and CSF measures of β-amyloid burden at an individual level suggests that these measures may not be interchangeable in assessing amyloid status nor response to amyloid targeting therapies.

Regional variations in cortical vs. striatal PiB PET signal in relation to EYO were also seen across pathogenic variants, with most groupings showing similar cortical and striatal PiB PET signal, but others showing striatal or cortical predominant patterns. At least one prominent prior report[16] has suggested that β-amyloid accumulation in autosomal dominant Alzheimer's disease may start in the striatum. Interestingly, this previous study used data from two families with mutations in the PSEN1 transmembrane domain 8. This result is consistent with what is observed here, as PSEN1 transmembrane domain 8 was among two groupings that showed a striatal predominant pattern of PiB PET signal. However, this pattern was the exception rather than the rule, as the observations here suggest that cortical and striatal PiB signal rise in tandem for many autosomal dominant Alzheimer's disease variants, but that some pathogenic variants may demonstrate cortical or striatal predominant patterns.

While measures of CSF Aβ and β-amyloid PET are sometimes used interchangeably to assess "amyloid positivity"[21], the results here provide a striking demonstration that these two measures can diverge substantially (Figure 4, Figure S3-S4). More work is needed to determine the biologic processes that may alter the commonly observed relationship between CSF and PET based measures of β-amyloid burden, as this divergence may have relevance for the clinical and research interpretations of these measures of Alzheimer's disease pathology. This divergence may be due to variant-dependent differences in the production of aggregation-prone Aβ species (especially Aβ42 and 43) relative to less aggregation, shorter fragments. We observed here that variant-dependent variations in β-amyloid PET signal across the autosomal dominant Alzheimer's disease course do not necessarily correlate with functional decline and are not easily explained by CSF Aβ42/40 ratio measured *in vivo* from these same individuals. However, while prior work indicates that most autosomal dominant Alzheimer's disease causing variants lead to increased production of Aβ42 relative to Aβ40[4], the mean age of onset for particular PSEN1 pathogenic variants was not correlated with the *in vitro* production of Aβ42/40 for that variant[8], suggesting that the Aβ42/40 ratio by itself may not be sufficient to characterize the pathogenicity of a particular disease-causing variant. Accordingly, assessment of other Aβ fragments (especially Aβ38 and 43) may be needed to better characterize the pathogenicity of individual disease-causing variants. In contrast, more recent work assessing plasma concentrations of Aβ38, 40, and 42 in an autosomal dominant Alzheimer's disease sample suggests that *in vivo* measures of γ-secretase function are moderately correlated with age of onset within *PSEN1* variant carriers[19]. In addition to examining this issue in a broader set of variants, aspects of γ-secretase function apart from APP processing need to be considered, including alterations in the processing of other γ-secretase substrates and effects on calcium homeostasis[7,10,22,23].

The disconnect between CSF and PET measures of Aβ observed in some variant groupings also raises the intriguing possibility that certain pathogenic variants may aggregate amyloid pathology in forms[24-26] that are differentially detectable by amyloid PET. While further pathologic characterization is needed to address this possibility, this hypothesis would be consistent with what has been seen in a more dramatic form with the *APP* E693G (Arctic) mutation, where amyloid deposits appear not to be detectable by PiB, even in advanced states of impairment[27,28]. Alternatively, it may be that the "true" burden of pathologic amyloid across pathogenic variants may itself be variable, despite similarities in rates of functional decline. Regardless of the cause, the potential for discordance between CSF and PET measures of β-amyloid burden itself raises questions for the interchangeable use of these measures in A/T/N staging and as surrogate markers of disease progression in both sporadic and autosomal dominant Alzheimer's disease. From a more mechanistic perspective, the high degree of variability in relationships between CSF Aβ42 and the CSF Aβ42/40 ratio with β-amyloid PET observed here also raises questions regarding the common assumption that CSF Aβ levels are reduced due to sequestration of these peptides within insoluble β-amyloid plaques.

Strengths of this study include a large sample size and greater diversity of autosomal dominant Alzheimer's disease pathogenic variants relative to other studies in the literature. Additionally, the availability of longitudinal PiB PET data allowed for the verification of cross-sectional patterns in longitudinal data for the codon-based grouping. The need to combine individual variants into groups based on the affected protein domain or location within *PSEN1* (relative to codon 200) reduced the number of comparisons, allowed for a broader range of EYO to be represented, and allowed for potentially more stable statistical estimates due to a greater number of data points within each grouping. Additionally, combining variants into groups likely reduces the impact of polygenic effects related to family-membership on the results, as all groupings had at least 2 families contributing data (and the majority of groupings had greater than 10 families represented; Supplemental Table 1 and 2). This is particularly true for the *PSEN1* codon 200 based groupings, each of which had more than 30 families represented. Consistent with this, adjusting for an IGAP-derived polygenic risk score at an individual level did not account for the observed associations between either variant-grouping relative to EYO and β-amyloid PET signal (Supplemental Table 4). Conversely, the grouping of variants may diminish variant-dependent effects by causing variants with dissimilar effects on fibrillar β-amyloid to be included in the same group by virtue of their proximity within the affected gene. However, grouping dissimilar variants together should bias the results away from seeing a significant effect of variant grouping, rather than the observed pattern of robust, variant grouping associated effects.

Several other limitations are also important to consider. Though all domain-based groups had at least 14 mutation carriers contributing data, more statistical power within a particular grouping may be needed to observe subtle variant-dependent effects. Related to this, while the potential effects of family membership on the results here were addressed in sensitivity analyses and by including family as a random effect in statistical models, fully eliminating the possibility of family membership effects will require larger samples in which the same pathogenic variants are present in different genetic and

environmental backgrounds. This initial examination of variant-dependent variability in β-amyloid burden in autosomal dominant Alzheimer's disease made use of variant categories defined *a priori* based on prior literature (codon 200 grouping) or based on the portion of the protein impacted by the underlying pathogenic variant (domain-based grouping). While the biological implications of each pathogenic variant likely differ based partially on location affected within the resulting protein (e.g., within a transmembrane vs. cytoplasmic domain), further work is necessary to generate data- and biochemically-driven variant groupings that are likely to better cluster biologically similar variants than the groupings used in the present report. Lastly, it will also be important to extend this work into other imaging and biochemical measures in DIAN, and particularly to examine potential variant-dependent changes in biofluid and PET measures of tau pathology, when sufficient data of this type becomes available.

Despite these limitations, the results here provide strong evidence that the underlying pathogenic variant is an important determinant of the topography and burden of β-amyloid deposition in autosomal dominant Alzheimer's disease, and consequently important to the success of clinical trials of amyloid-focused treatments in this population. Relevant to both sporadic and autosomal dominant Alzheimer's disease, understanding the underlying biology that may cause measures of CSF Aβ to diverge strongly from PET measures of β-amyloid burden may help refine the use of these measures as surrogate markers of Alzheimer's disease pathologic progression. More fundamentally, the observed discordance between apparent β-amyloid burden and stage of disease in autosomal dominant Alzheimer's disease underscores that, while PET and CSF measures of β-amyloid measures are critically valuable biomarkers in Alzheimer's disease clinical and translational research, these widely-used biomarkers may not comprehensively and unerringly reflect the essential, amyloid-related pathobiological processes that drive Alzheimer's disease progression at an individual level.

Supplemental Methods:

Choice of Pathogenic Variants:

Using previously described methods[29], potentially pathogenic *APP*, *PSEN1*, and *PSEN2* variants were filtered to retain those classified as probably pathogenic based on committee evaluation integrating multiple criteria: 1) variant segregation with clinical or autopsy-confirmed Alzheimer's disease; 2) variant carrier biomarker data; 3) variant frequency in gnomAD and ExAC population databases; 4) pathogenic status of other variants affecting the same amino acid residue; 5) amino acid residue conservation between *PSEN1* and *PSEN2*; 6) variant effect on amyloid beta processing in cell culture models. As described previously[29], only variants judged to have a high likelihood of being pathogenic were included in the present analyses.

Sensitivity Analyses Assessing Family Membership Effects:

In addition to including family membership as a random effect in all statistical models in the main text, we performed several additional analyses to assess the possible influence of family membership on the foregoing analyses. First, we calculated influence metrics (Cook's distance) for each family in models determining variant-dependent effects on cortical PiB PET signal. Cook's distance values were generally low, with a mean value of 0.02 and an SD of 0.029. There were 7 families with Cook's d values 1 SD or greater from the mean ($d \geq 0.049$; Supplemental Figure 7). Excluding these 7 families did not change the results of this analysis (Supplemental Table 4). Likewise, excluding all PSEN2 or APP pathogenic variant carriers also had little impact on models examining variant dependent variations in amyloid PET (Supplemental Table 4).

As individuals within the same family may share polygenic risk factors for Alzheimer's disease, we used previously described methods[30] to calculate a weighted polygenic risk score (PRS) for each participant based on data from International Genomics of Alzheimer's Project (IGAP). In brief, DIAN participants were genotyped with the Illumina 610 or Omni-express chip (Illumina, San Diego, CA, USA), followed by imputation with SHAPEIT/IMPUTE2, using the 1000 Genomes Project as a reference panel. We tested the resulting PRS as covariates in models examining variant grouping dependent effects on amyloid PET. Including PRS as a covariate or excluding pathogenic variant carriers with 1SD greater than the mean PRS did not alter associations between domain-based or codon-based groupings and amyloid PET. Similarly, excluding individuals carrying an *APOE* ε4 or an *APOE* ε2 allele also did not impact these models (Supplemental Table 4).

Acknowledgements: Data collection and sharing for this project was supported by the Dominantly Inherited Alzheimer Network (DIAN, UF1AG032438) funded by the NIA, the German Center for Neurodegenerative Diseases (DZNE), and partial support by the Research and Development, grants for Dementia from Japan Agency for Medical Research and Development. NJM gratefully acknowledges support from an Alzheimer's Association Research Training Fellowship. This manuscript has been reviewed by DIAN Study investigators for scientific content and consistency of data interpretation with

previous DIAN Study publications. The authors acknowledge the altruism of the participants and their families and contributions of the DIAN research and support staff at each of the participating sites for their contributions to this study.

Data Sharing Statement: Biomarker and cognitive data from the DIAN Observational Study is available by request at https://dian.wustl.edu/our-research/observational-study/dian-observational-study-investigator-resources/data-request-terms-and-instructions/

Declaration of Interest:
JPC has served on medical advisory boards for Otsuka Pharmaceuticals and Humana Healthcare. There are no conflicts.

APS has served on medical advisory boards for Janssen Pharmaceuticals and Biogen. There are no conflicts.

SMS reports consulting to Eisai, Novartis, Genentech, F. Hoffmann-La Roche, Ltd, Gemvax, Avid Radiopharmaceuticals and Eli Lilly and Company. He also serves on the steering committees for major biomarker and clinical trials and consortia such as ADNI, DIAN, ACTC, GAP-NET and LEADS and he is a Project Arm Leader for the DIAN-TU study. There are no conflicts.

WEK is a co-inventor of PiB and, as such, has a financial interest in a license agreement held by GE Healthcare and the University of Pittsburgh based on the PiB PET technology used in this manuscript. GE Healthcare provided no grant support for this study and had no role in the design or interpretation of results or preparation of this manuscript. There are no conflicts.

AMF has received research funding from the National Institutes of Health /National Institute on Aging, Biogen, Centene, Fujirebio, and Roche Diagnostics. She is a member of the scientific advisory boards for Roche Diagnostics, Genentech, and AbbVie and also consults for Araclon/Grifols, DiademRes, DiamiR, and Otsuka Pharmaceuticals. There are no conflicts.

RJB has equity ownership interest in C2N Diagnostics and receives royalty income based on technology (stable isotope labeling kinetics and blood plasma assay) licensed by Washington University to C2N Diagnostics. He receives income from C2N Diagnostics for serving on the scientific advisory board. Washington University, with RJB as co-inventor, has submitted the US nonprovisional patent application “Cerebrospinal fluid (CSF) tau rate of phosphorylation measurement to define stages of Alzheimer’s disease and monitor brain kinases/phosphatases activity.” He has received honoraria from Janssen and Pfizer as a speaker, and from Merck and Pfizer as an advisory board member. He has been an invited speaker, advisory board member, and consultant for F. Hoffman La Roche, Ltd., an invited speaker and consultant for AC Immune and Janssen, and a consultant for Amgen and Eisai. There are no conflicts.

AMG has consulted for Eisai, Biogen, Pfizer, AbbVie, Cognition Therapeutics, and GSK. She also served on the Scientific Advisory Board of Denali Therapeutics (2015–2018). There are no conflicts.

RAS and KAJ are involved in public-private partnership clinical trials sponsored by the NIH and Eli Lilly and Co., who owns the distribution rights to Flortaucipir (AV-1451), but they do not have any personal financial relationship with Eli Lilly. There are no conflicts.

NGR reports grants from Biogen, grants from Abbvie, grants from Lilly outside the submitted work.

SAS, YJS EM, LL, BH, BTE, NJM, TLSB, RF, JCM, CDF, KPS, JL, JHL, WEK, MJ, AH, JMN, NGR, MVF, HM, SMS, CC, SB, CLM, RJP, AER, CMK, EM CX, BAG, TM, NF, PRS report no conflicts.

Author contributions:
Literature Search: JPC, SAS
Study Design: JPC, SAS, EM, BH, RAS, KAJ
Data Collection: JPC, SAS, EM, APS, BH, NJM, RF, CDF, KPS, JL, SB, JHL, MJ, AH, JMN, NGR, HM, SMS, CLM, RM, CMK, CX, CC, BAG, TM, TLSB, NF, PRS, AER, BTE, MVF, YJS, AMF, AG, RJB
Data analysis: JPC, SAS, EM, BH, APS
Data Interpretation: JPC, SAS, EM, APS, WEK, LL, AG, KAJ, RAS
Figures: JPC, SAS, APS
Manuscript Writing: JPC, SAS, EM, RAS
Manuscript Critical Review: JPC, SAS, EM, APS, LL, BH, NJM, RF, CDF, KPS, JL, SB, JHL, WEK, MJ, AH, JMN, NGR, HM, SMS, CC, CLM, RM, AER, BTE, MVF, YJS, CMK, CX, CC, BAG, TM, TLSB, NF, JCM, PRS, AMF, AG, RJB, KAJ, RAS
Verified Underlying Data: JPC, SAS, APS

References:

1. Ryman DC, Acosta-Baena N, Aisen PS, et al. Symptom onset in autosomal dominant Alzheimer disease: A systematic review and meta-analysis. *Neurology* 2014; **83**(3): 253-60.
2. Bateman RJ, Xiong C, Benzinger TLS, et al. Clinical and Biomarker Changes in Dominantly Inherited Alzheimer's Disease. *The New England journal of medicine* 2012; **367**(9): 795-804.
3. Reiman EM, Quiroz YT, Fleisher AS, et al. Brain imaging and fluid biomarker analysis in young adults at genetic risk for autosomal dominant Alzheimer's disease in the presenilin 1 E280A kindred: a case-control study. *The Lancet Neurology* 2012; **11**(12): 1048-56.
4. Borchelt DR, Thinakaran G, Eckman CB, et al. Familial Alzheimer's Disease–Linked Presenilin 1 Variants Elevate Aβ1–42/1–40 Ratio In Vitro and In Vivo. *Neuron* 1996; **17**(5): 1005-13.
5. Paterson RW, Gabelle A, Lucey BP, et al. SILK studies - capturing the turnover of proteins linked to neurodegenerative diseases. *Nat Rev Neurol* 2019; **15**(7): 419-27.

6. Potter R, Patterson BW, Elbert DL, et al. Increased in Vivo Amyloid- 42 Production, Exchange, and Loss in Presenilin Mutation Carriers. *Science Translational Medicine* 2013; **5**(189): 189ra77-ra77.
7. Selkoe DJ, Hardy J. The amyloid hypothesis of Alzheimer's disease at 25 years. *EMBO Molecular Medicine* 2016; **8**(6): 595-608.
8. Sun L, Zhou R, Yang G, Shi Y. Analysis of 138 pathogenic mutations in presenilin-1 on the in vitro production of Aβ42 and Aβ40 peptides by γ-secretase. *Proceedings of the National Academy of Sciences of the United States of America* 2016: 201618657.
9. Scheuner D, Eckman C, Jensen M, et al. Secreted amyloid β–protein similar to that in the senile plaques of Alzheimer's disease is increased in vivo by the presenilin 1 and 2 and APP mutations linked to familial Alzheimer's disease. *Nature Medicine* 1996; **2**(8): 864-70.
10. Bentahir M, Nyabi O, Verhamme J, et al. Presenilin clinical mutations can affect gamma-secretase activity by different mechanisms. *Journal of Neurochemistry* 2006; **96**(3): 732-42.
11. Chávez-Gutiérrez L, Bammens L, Benilova I, et al. The mechanism of γ-Secretase dysfunction in familial Alzheimer disease. *The EMBO Journal* 2012; **31**(10): 2261-74.
12. Wolfe MS. Dysfunctional γ-Secretase in Familial Alzheimer's Disease. *Neurochemical Research* 2019; **44**(1): 5-11.
13. Su Y, Blazey TM, Snyder AZ, et al. Partial volume correction in quantitative amyloid imaging. *Neuroimage* 2015; **107**: 55-64.
14. Mann DMA, Pickering-Brown SM, Takeuchi A, Iwatsubo T. Amyloid Angiopathy and Variability in Amyloid β Deposition Is Determined by Mutation Position in Presenilin-1-Linked Alzheimer's Disease. 2001; **158**(6): 2165-75.
15. Ringman JM, Monsell S, Ng DW, et al. Neuropathology of Autosomal Dominant Alzheimer Disease in the National Alzheimer Coordinating Center Database. 2016; **75**(3): 284-90.
16. Klunk WE, Price JC, Mathis CA, et al. Amyloid deposition begins in the striatum of presenilin-1 mutation carriers from two unrelated pedigrees. *Journal of Neuroscience* 2007; **27**(23): 6174-84.
17. Villemagne VL, Ataka S, Mizuno T, et al. High Striatal Amyloid β-Peptide Deposition Across Different Autosomal Alzheimer Disease Mutation Types. *Archives of Neurology* 2009; **66**(12): 1537-44.
18. Cohen AD, McDade E, Christian B, et al. Early striatal amyloid deposition distinguishes Down syndrome and autosomal dominant Alzheimer's disease from late-onset amyloid deposition. *Alzheimer's & Dementia* 2018; **14**(6): 743-50.
19. O'Connor A, Pannee J, Poole T, et al. Plasma Aβ ratios in autosomal dominant Alzheimer's disease: the influence of genotype. Cold Spring Harbor Laboratory; 2021.
20. Swanson C, Kanekiyo M, Kaplow J, et al. Plasma Aβ 42:40 Ratio Tracks with Changes in Brain Amyloid PET SUVr in the Core and Open Label Extension of the Phase 2 Proof of Concept Study BAN2401-G000-201 Following Treatment with Lecanemab in Subjects with Early Alzheimer's Disease. *Alzheimer's Association International Conference, Denver, USA* 2021.
21. Jack CR, Jr., Bennett DA, Blennow K, et al. NIA-AA Research Framework: Toward a biological definition of Alzheimer's disease. *Alzheimers Dement* 2018; **14**(4): 535-62.
22. Xia D, Watanabe H, Wu B, et al. Presenilin-1 Knockin Mice Reveal Loss-of-Function Mechanism for Familial Alzheimer's Disease. *Neuron* 2015; **85**(5): 967-81.
23. Tu H, Nelson O, Bezprozvanny A, et al. Presenilins Form ER Ca2+ Leak Channels, a Function Disrupted by Familial Alzheimer's Disease-Linked Mutations. *Cell* 2006; **126**(5): 981-93.
24. Maarouf CL, Daugs ID, Spina S, et al. Histopathological and molecular heterogeneity among individuals with dementia associated with Presenilin mutations. *Molecular Neurodegeneration* 2008; **3**(1): 20.
25. Miravalle L, Calero M, Takao M, Roher AE, Ghetti B, Vidal R. Amino-Terminally Truncated Aβ Peptide Species Are the Main Component of Cotton Wool Plaques†. *Biochemistry* 2005; **44**(32): 10810-21.
26. Mann DMA, Takeuchi A, Sato S, et al. Cases of Alzheimer's disease due to deletion of exon 9 of the presenilin-1 gene show an unusual but characteristic β-amyloid pathology known as 'cotton wool' plaques. *Neuropathology and Applied Neurobiology* 2001; **27**(3): 189-96.
27. Scholl M, Wall A, Thordardottir S, et al. Low PiB PET retention in presence of pathologic CSF biomarkers in Arctic APP mutation carriers. *Neurology* 2012; **79**(3): 229-36.

28. Nilsberth C, Westlind-Danielsson A, Eckman CB, et al. The 'Arctic' APP mutation (E693G) causes Alzheimer's disease by enhanced Aβ protofibril formation. *Nature Neuroscience* 2001; **4**(9): 887-93.
29. Hsu S, Gordon BA, Hornbeck R, et al. Discovery and validation of autosomal dominant Alzheimer's disease mutations. *Alzheimers Res Ther* 2018; **10**(1): 67.
30. Cruchaga C, Del-Aguila JL, Saef B, et al. Polygenic risk score of sporadic late-onset Alzheimer's disease reveals a shared architecture with the familial and early-onset forms. *Alzheimer's & Dementia : the Journal of the Alzheimer's Association* 2018; **14**(2): 205-14.

Figure Legends:

Figure 1: *Categorization of autosomal dominant Alzheimer's disease pathogenic variants:* Data from 347 participants in the DIAN observational study with available PiB-PET and CSF measures were used in the analysis. The locations of the 62 unique pathogenic variants in PSEN1, PSEN2, and APP in this dataset are represented in panels A-C. As this dataset contained a large number of unique pathogenic variants, individual variants in PSEN1, PSEN2, and APP were categorized (Panel D) based on the affected protein domain (Dataset A) or by whether pathogenic variants were before or after codon 200 in PSEN1 (Dataset B). In dataset A, only variant categories with > 10 pathogenic variant carriers were retained as distinct groups. Carriers from variant groupings with fewer than 10 participants were retained as Ungrouped carriers. For Dataset B, only PSEN1 pathogenic variant carriers and their family members were retained in the analysis. Further detail for variant groupings is shown in Supplemental Table 1 and 2.

Figure 2: *Trajectories of Amyloid Burden Across EYO:* Amyloid burden in autosomal dominant Alzheimer's disease pathogenic variant carriers (red) and non-carriers (blue) as assessed by PiB PET (A; cortical mean) and CSF Aβ42 (B). Gray dashed line corresponds to age of expected symptom onset. In both PET and CSF assessments, evidence of increased amyloid burden is seen in pathogenic variant carriers compared to non-carriers at least 10 years prior to symptom onset. Individual data points suggest substantial inter-individual variation in amyloid burden measured by PiB PET (C) and by CSF Aβ42 (D) in pathogenic variant carriers (only carriers shown in C and D; level of impairment coded with shapes and colors using the Clinical Dementia Rating global score - CDR).

Figure 3: *Amyloid Burden and Functional Decline Considering Variant Groupings:* Trajectories of PiB PET (A,D), CSF Aβ42 (B, E), and Clinical Dementia Rating (CDR) sum of boxes (C,F) across variant groupings. In panels A-C, individual variants were categorized according to the protein domain affected by the underlying genetic variation. In panels D-F, PSEN1 pathogenic variant carriers were grouped based on whether the identified variant in PSEN1 was before or after codon 200. No significant differences between variant groupings were observed in CSF Aβ42 or in CDR sum of boxes (panels B, C, E, and F), but significant variant-dependent variations in amyloid PET signal were observed using both the domain- and codon-based groupings (A,D; Supplemental Figure 2). * denotes FDR corrected $p \leq 0.05$ for each variant grouping by EYO interaction compared to all other pathogenic variant carriers; † denotes FDR corrected $p \leq 0.0001$ for carriers of PSEN1 variants prior to codon 200 compared to those carriers of variants post codon 200.

Figure 4: *Variant-dependent Variations in PiB PET: Illustrative Cases:* PiB-PET images from autosomal dominant Alzheimer's disease pathogenic variant carriers starting from early, pre-symptomatic stages of disease (left) to later stages with recognized clinical impairment (right) as measured by the global Clinical Dementia Rating (CDR) and CDR Sum of Boxes. CSF Aβ42, cortical and striatal mean PiB values, and variant grouping are shown below each image (Transmembrane Domain: TM; Estimated Years to Symptom Onset: EYO). These images were chosen to demonstrate the heterogeneity present in β-amyloid measures across the course of autosomal dominant Alzheimer's disease. Examples of striatal predominant patterns are shown in Supplemental Figure 5.

Figure 5: *Longitudinal PiB PET:* Individual pathogenic variant carriers are plotted in panel A, with each point representing a PiB PET measurement and lines connecting observations from the same participant. To examine how amyloid PET signal may vary longitudinally by stage of disease, variant carriers were separated into early asymptomatic, late asymptomatic, and impaired phases of autosomal dominant Alzheimer's disease, and the yearly change in PiB PET signal was calculated from the available longitudinal data (panel B). P-values shown are FDR corrected.

Figure 6: *Variant-dependent Variability in Regional Amyloid Burden:* Trajectories of striatal mean PiB SUVR across EYO with pathogenic variants grouped according to affected protein domain (A) or in PSEN1 carriers with genetic variants before or after codon 200 (B). Individual variant categories from panel A are depicted in panels C-K, with cortical mean shown in colored solid lines and striatal mean in gray dashed lines. + denotes $p \leq 0.05$ for main effect of variant grouping relative to other pathogenic variant carriers; † indicates $p \leq 0.0005$ for the presence of a codon-based grouping by EYO interaction; * indicates $p \leq 0.05$ for comparison of cortical to striatal PiB PET SUVR within each variant grouping . P-values are FDR corrected.

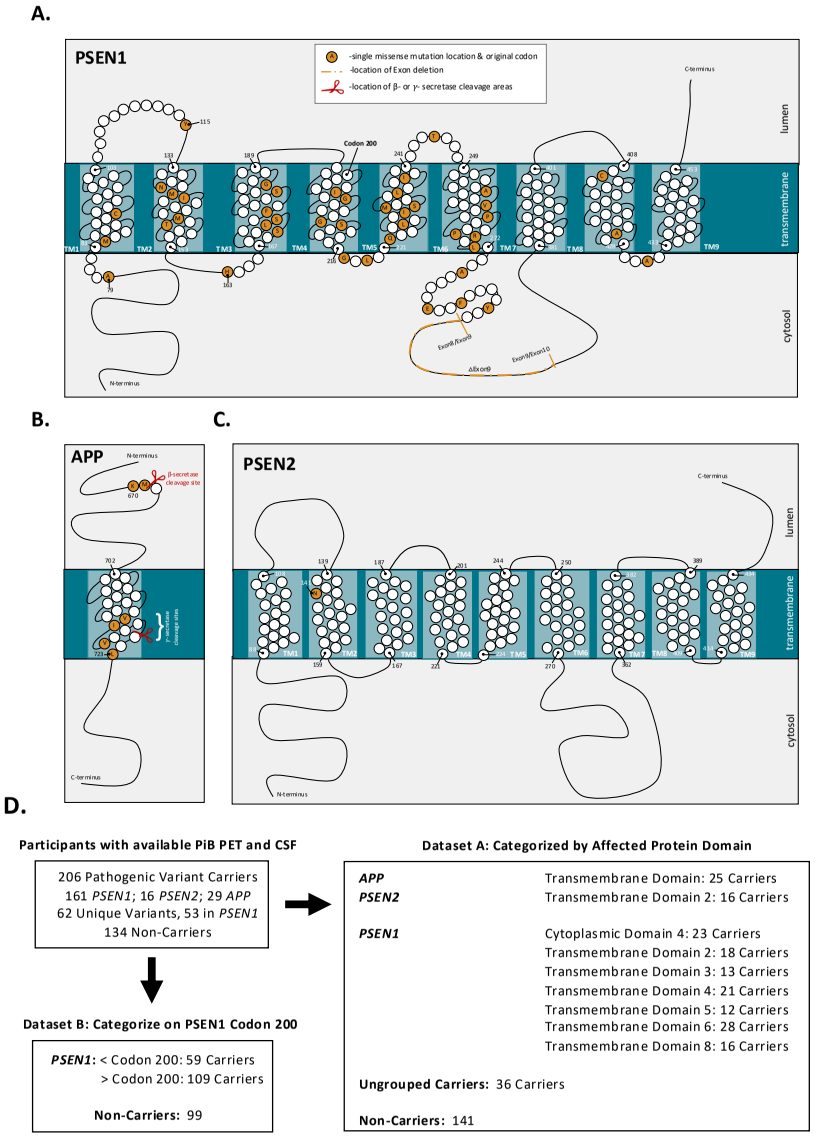

Figure 1: *Categorization of autosomal dominant Alzheimer's disease pathogenic variants:* Data from 347 participants in the DIAN observational study with available PiB-PET and CSF measures were used in the analysis. The locations of the 62 unique pathogenic variants in PSEN1, PSEN2, and APP in this dataset are represented in panels A-C. As this dataset contained a large number of unique pathogenic variants, individual variants in PSEN1, PSEN2, and APP were categorized (Panel D) based on the affected protein domain (Dataset A) or by whether pathogenic variants were before or after codon 200 in PSEN1 (Dataset B). In dataset A, only variant categories with > 10 pathogenic variant carriers were retained as distinct groups. Carriers from variant groupings with fewer than 10 participants were retained as Ungrouped carriers. For Dataset B, only PSEN1 pathogenic variant carriers and their family members were retained in the analysis. Further detail for variant groupings is shown in Supplemental Table 1 and 2.

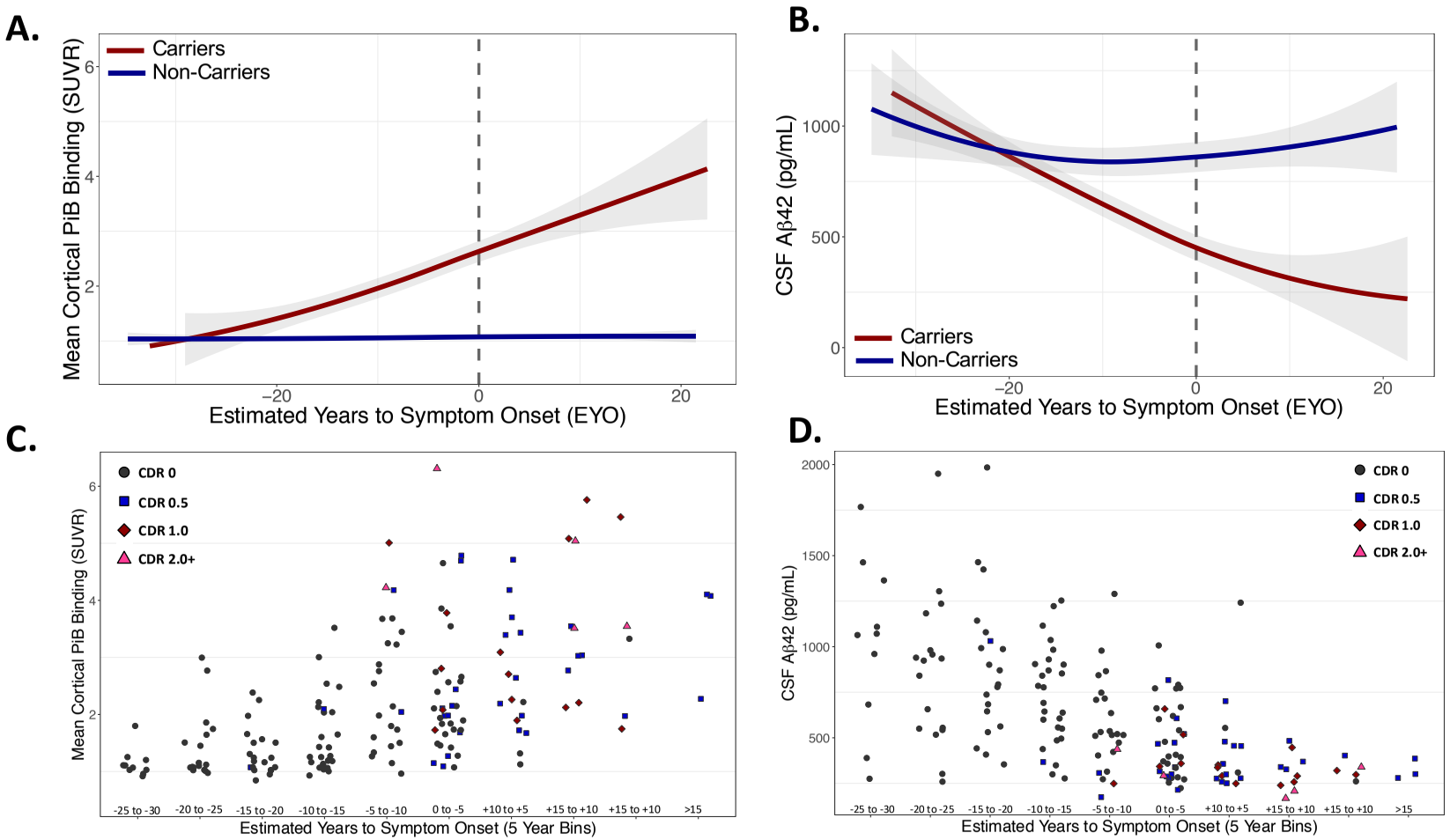

Figure 2: *Trajectories of Amyloid Burden Across EYO:* Amyloid burden in autosomal dominant Alzheimer's disease pathogenic variant carriers (red) and non-carriers (blue) as assessed by PiB PET (A; cortical mean) and CSF Aβ42 (B). Gray dashed line corresponds to age of expected symptom onset. In both PET and CSF assessments, evidence of increased amyloid burden is seen in pathogenic variant carriers compared to non-carriers at least 10 years prior to symptom onset. Individual data points suggest substantial inter-individual variation in amyloid burden measured by PiB PET (C) and by CSF Aβ42 (D) in pathogenic variant carriers (only carriers shown in C and D; level of impairment coded with shapes and colors using the Clinical Dementia Rating global score - CDR).

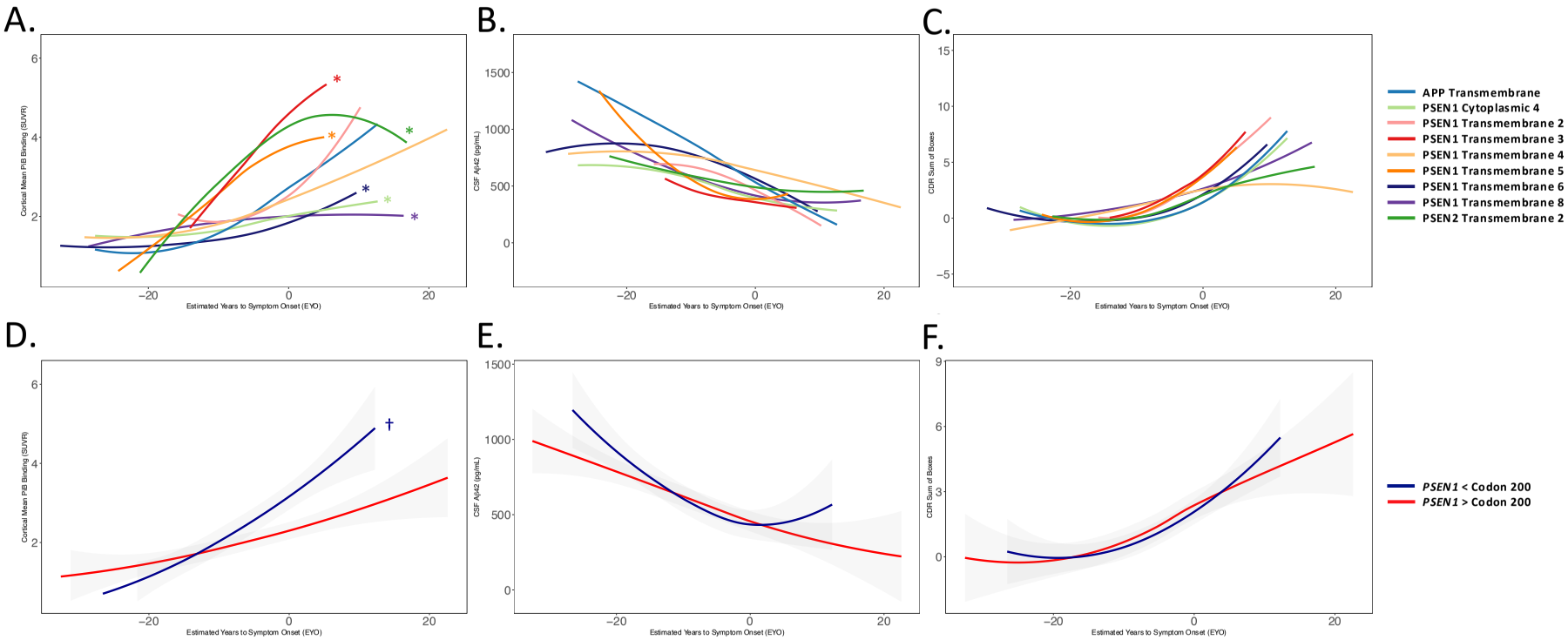

Figure 3: *Amyloid Burden and Functional Decline Considering Variant Groupings:* Trajectories of PiB PET (A,D), CSF Aβ42 (B, E), and Clinical Dementia Rating (CDR) sum of boxes (C,F) across variant groupings. In panels A-C, individual variants were categorized according to the protein domain affected by the underlying genetic variation. In panels D-F, PSEN1 pathogenic variant carriers were grouped based on whether the identified variant in PSEN1 was before or after codon 200. No significant differences between variant groupings were observed in CSF Aβ42 or in CDR sum of boxes (panels B, C, E, and F), but significant variant-dependent variations in amyloid PET signal were observed using both the domain- and codon-based groupings (A,D; Supplemental Figure 2). * denotes FDR corrected $p \leq 0.05$ for each variant grouping by EYO interaction compared to all other pathogenic variant carriers; † denotes FDR corrected $p \leq 0.0001$ for carriers of PSEN1 variants prior to codon 200 compared to those carriers of variants post codon 200.

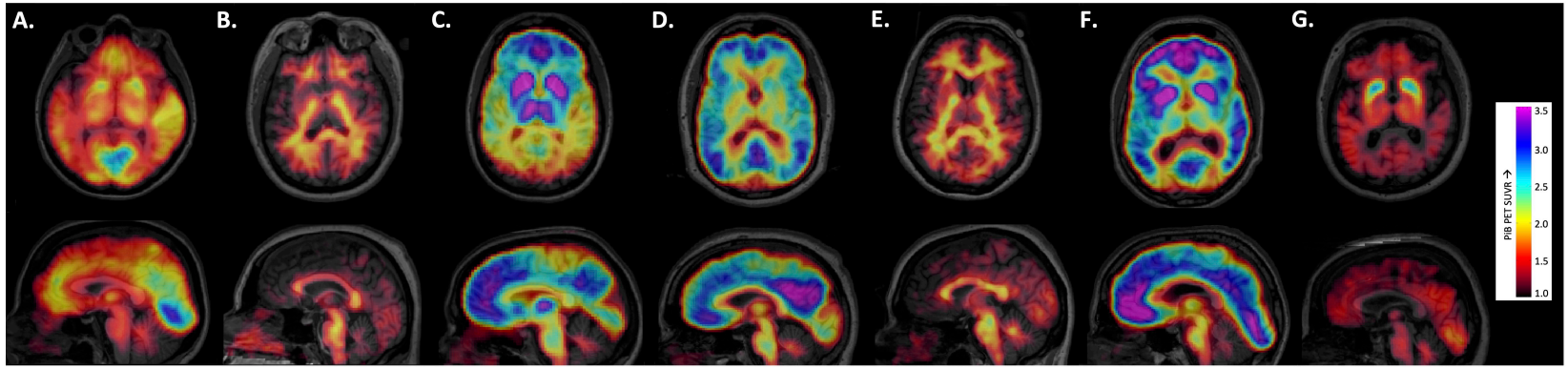

Figure 4: *Variant-dependent Variations in PiB PET: Illustrative Cases:* PiB-PET images from autosomal dominant Alzheimer's disease pathogenic variant carriers starting from early, pre-symptomatic stages of disease (left) to later stages with recognized clinical impairment (right) as measured by the global Clinical Dementia Rating (CDR) and CDR Sum of Boxes. CSF Aβ42, cortical and striatal mean PiB values, and variant grouping are shown below each image (Transmembrane Domain: TM; Estimated Years to Symptom Onset: EYO). These images were chosen to demonstrate the heterogeneity present in β-amyloid measures across the course of autosomal dominant Alzheimer's disease. Examples of striatal predominant patterns are shown in Supplemental Figure 5.

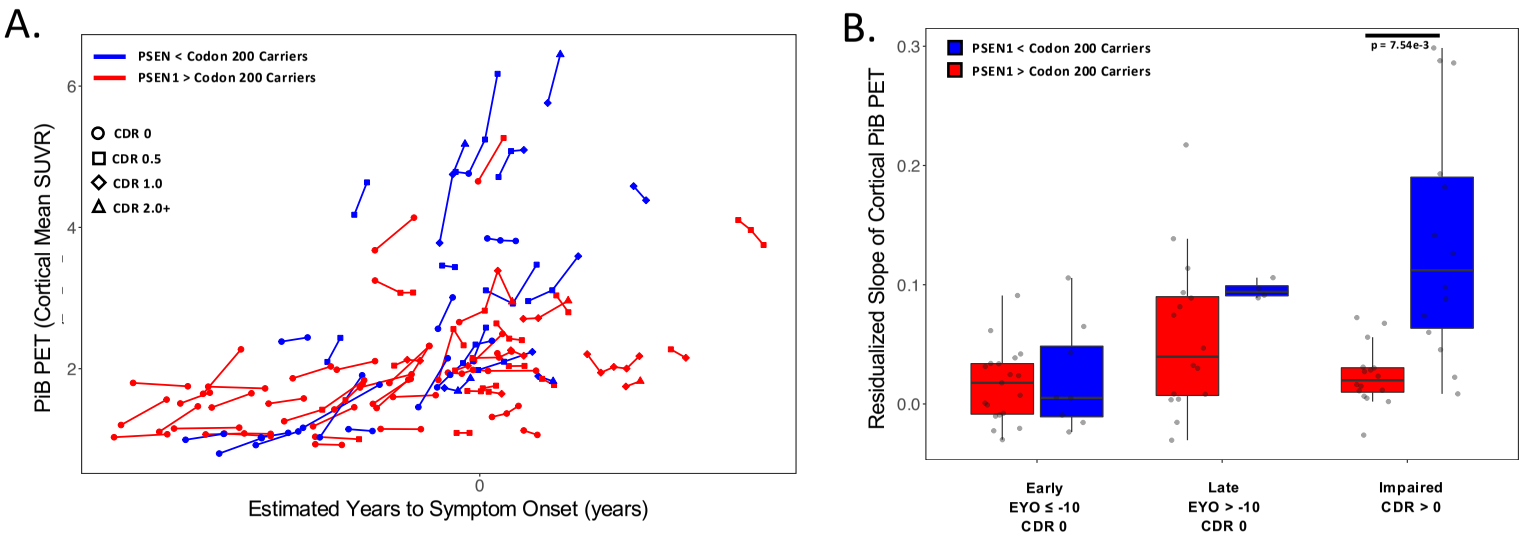

Figure 5: *Longitudinal PiB PET:* Individual pathogenic variant carriers are plotted in panel A, with each point representing a PiB PET measurement and lines connecting observations from the same participant. To examine how amyloid PET signal may vary longitudinally by stage of disease, variant carriers were separated into early asymptomatic, late asymptomatic, and impaired phases of autosomal dominant Alzheimer's disease, and the yearly change in PiB PET signal was calculated from the available longitudinal data (panel B). P-values shown are FDR corrected.

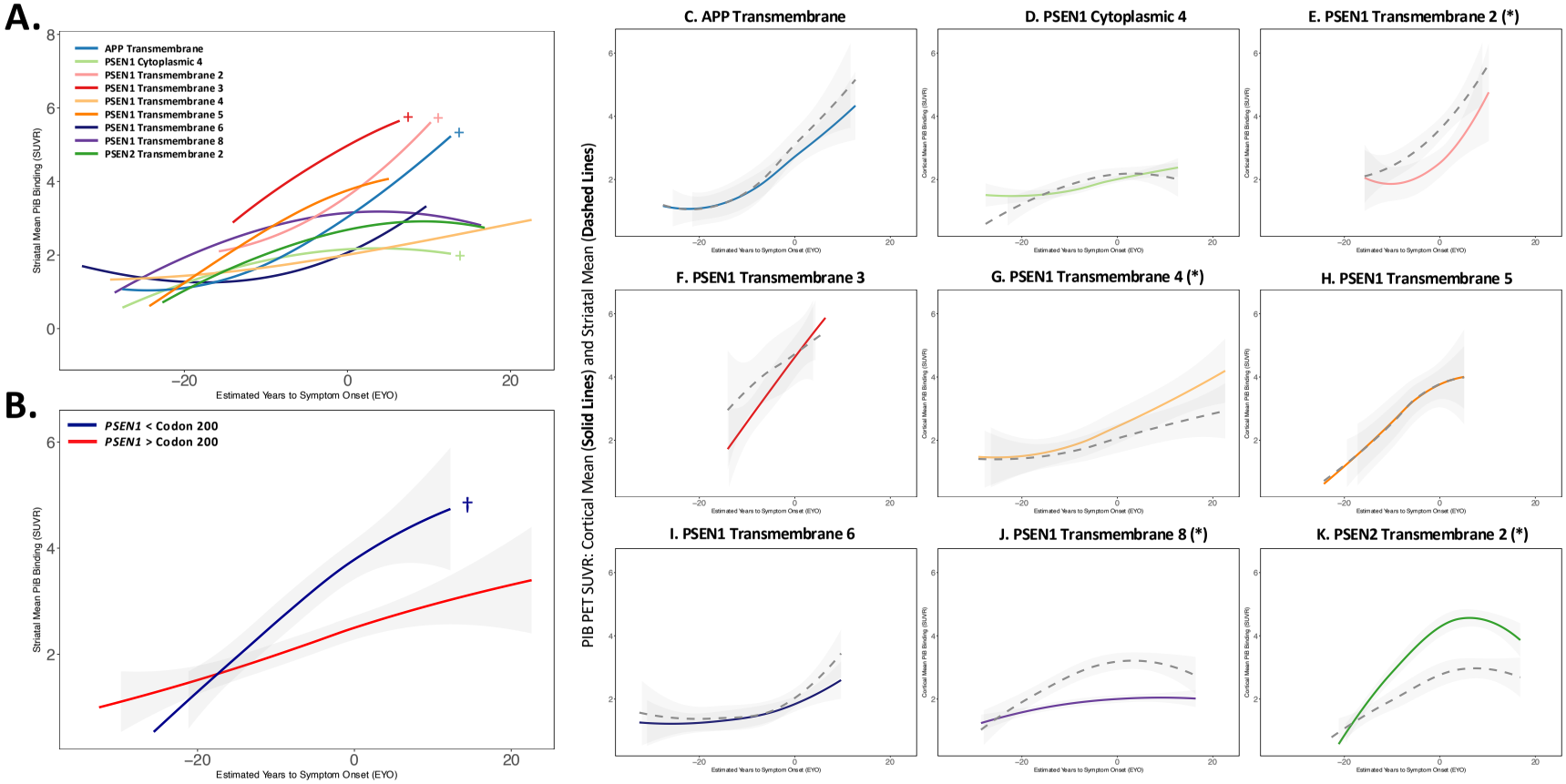

Figure 6: *Variant-dependent Variability in Regional Amyloid Burden:* Trajectories of striatal mean PiB SUVR across EYO with pathogenic variants grouped according to affected protein domain (A) or in PSEN1 carriers with genetic variants before or after codon 200 (B). Individual variant categories from panel A are depicted in panels C-K, with cortical mean shown in colored solid lines and striatal mean in gray dashed lines. + denotes $p \leq 0.05$ for main effect of variant grouping relative to other pathogenic variant carriers; † indicates $p \leq 0.0005$ for the presence of a codon-based grouping by EYO interaction; * indicates $p \leq 0.05$ for comparison of cortical to striatal PiB PET SUVR within each variant grouping . P-values are FDR corrected.

Supplemental Table 1: Demographics and Family Representation in Pathogenic Variant Groupings						
Dataset A:	*# of Pathogenic Variant Carriers/Families*	*# Variants*	*Variants Represented in Domain-Based Grouping*	Baseline EYO (mean years/SD)	Baseline Age (mean years/SD)	Familial Age of Onset (mean years/SD)
APP Transmembrane Domain	25 / 17	6	APP:p.Val715Ala, APP:p.Ile716Phe, APP:p.Ile716Val, APP:p.Val717Ile, APP:p.Val717Leu, APP:p.Leu723Arg	-10.52/11.69	37.72/10.95	48.24/7.68
PSEN2 Transmembrane Domain 2	16 / 2	1	PSEN2:p.Asn141Ile	-11.53/10.09	38.62/9.93	50.16/NA
PSEN1 Cytoplasmic Domain 4	23 / 9	6	PSEN1:p.Ala275Val, PSEN1:p.Glu280Ala, PSEN1:p.Glu280Gly, PSEN1:p.Phe283Leu, PSEN1:p.Tyr288His, PSEN1:exon9del	-6.67/9.05	34.35/8.11	41.02/4.36
PSEN1 Transmembrane Domain 2	18 / 13	8	PSEN1:p.Asn135Ser, PSEN1:p.Asn135Tyr, PSEN1:p.Ile143Thr, PSEN1:p.Met139Ile, PSEN1:p.Met146Ile, PSEN1:p.Met146Leu, PSEN1:p.Met146Val, PSEN1:p.Thr147Ile	-5.50/7.20	32.11/6.27	37.61/6.28
PSEN1 Transmembrane Domain 3	13/ 7	6	PSEN1:p.Ser169Leu, PSEN1:p.Ser170Phe, PSEN1:p.Leu171Pro, PSEN1:p.Phe176Val, PSEN1:p.Ser178Pro, PSEN1:p.Glu184Asp	-6.10/6.13	35.46/8.17	41.56/6.81
PSEN1 Transmembrane Domain 4	21 /14	5	PSEN1:p.Ile202Phe, PSEN1:p.Gly206Ala, PSEN1:p.Gly209Glu, PSEN1:p.Gly209Val, PSEN1:p.Ser212Tyr	-6.86/13.12	43.90/10.86	50.77/8.00
PSEN1 Transmembrane Domain 5	12 / 10	8	PSEN1:p.Gln222His, PSEN1:p.Ile229Phe, PSEN1:p.Leu226Arg, PSEN1:p.Ser230Asn, PSEN1:p.Met233Leu, PSEN1:p.Met233Thr, PSEN1:p.Leu235Val, PSEN1:p.Ile238Met	-8.25/8.89	38.50/9.48	46.75/9.79
PSEN1 Transmembrane Domain 6	28 / 12	7	PSEN1:p.Ala260Gly, PSEN1:p.Ala260Val, PSEN1:p.Val261Phe, PSEN1:p.Pro264Leu, PSEN1:p.Pro267Leu, PSEN1:p.Arg269His, PSEN1:p.Leu271Val	-8.44/11.62	43.57/11.39	52.01/6.24
PSEN1 Transmembrane Domain 8	16 /4	2	PSEN1:p.Cys410Tyr, PSEN1:p.Ala426Pro	-7.24/13.26	37.00/11.71	44.24/5.56
Ungrouped Carriers	34 / 24	12	APP:p.Lys670_Met671delinsAsnLeu, APP:dupplication, PSEN1:p.Ala79Val, PSEN1:p.Met84Val, PSEN1:p.Cys92Ser, PSEN1:p.Phe105Leu, PSEN1:p.Tyr115His, PSEN1:p.His163Arg, PSEN1:p.Gly217Arg, PSEN1:p.Leu219Pro, PSEN1:p.Thr245Pro, PSEN1:p.Ala431Glu	-9.74/10.74	37.18/10.61	46.92/7.53
Dataset B:						
PSEN1 pathogenic variant prior to codon 200	54 / 35	20	*PSEN1* variants in blue (above)	-8.04/9.10	34.93/8.88	42.97/8.31
PSEN1 pathogenic variant after codon 200	107 / 55	33	*PSEN1* variants in red (above)	-7.30/11.10	39.66/10.91	46.96/7.92

Supplemental Table 2: Variant Coding DNA Reference Sequences

Gene	Variant gDNA consequence	Variant cDNA consequence	Variant protein consequence
APP	chr21:g.27269938_27269939delinsGA	c.2010_2011delinsTC	p.Lys670_Met671delinsAsnLeu
APP	chr21:g.27264101A>G	c.2144T>C	p.Val715Ala
APP	chr21:g.27264099T>C	c.2146A>G	p.Ile716Val
APP	chr21:g.27264099T>A	c.2146A>T	p.Ile716Phe
APP	chr21:g.27264096C>T	c.2149G>A	p.Val717Ile
APP	chr21:g.27264096C>G	c.2149G>C	p.Val717Leu
APP	chr21:g.27264077A>C	c.2168T>G	p.Leu723Arg
APP	-	-	dup
PSEN1	chr14:g.73683933G>A	c.1229G>A	p.Cys410Tyr
PSEN1	chr14:g.73685869G>C	c.1276G>C	p.Ala426Pro
PSEN1	chr14:g.73685885C>A	c.1292C>A	p.Ala431Glu
PSEN1	chr14:g.73637653C>T	c.236C>T	p.Ala79Val
PSEN1	chr14:g.73637667A>G	c.250A>G	p.Met84Val
PSEN1	chr14:g.73637691T>A	c.274T>A	p.Cys92Ser
PSEN1	chr14:g.73637730T>C	c.313T>C	p.Phe105Leu
PSEN1	chr14:g.73640278T>C	c.343T>C	p.Tyr115His
PSEN1	chr14:g.73640338A>T	c.403A>T	p.Asn135Tyr
PSEN1	chr14:g.73640339A>G	c.404A>G	p.Asn135Ser
PSEN1	chr14:g.73640352G>C	c.417G>C	p.Met139Ile
PSEN1	chr14:g.73640363T>C	c.428T>C	p.Ile143Thr
PSEN1	chr14:g.73640371A>C	c.436A>C	p.Met146Leu
PSEN1	chr14:g.73640371A>G	c.436A>G	p.Met146Val
PSEN1	chr14:g.73640373G>C	c.438G>C	p.Met146Ile
PSEN1	chr14:g.73640375C>T	c.440C>T	p.Thr147Ile
PSEN1	chr14:g.73653568A>G	c.488A>G	p.His163Arg
PSEN1	chr14:g.73653586C>T	c.506C>T	p.Ser169Leu
PSEN1	chr14:g.73653589C>T	c.509C>T	p.Ser170Phe
PSEN1	chr14:g.73653592T>C	c.512T>C	p.Leu171Pro
PSEN1	chr14:g.73653606T>G	c.526T>G	p.Phe176Val
PSEN1	chr14:g.73653612T>C	c.532T>C	p.Ser178Pro
PSEN1	chr14:g.73659355A>C	c.552A>C	p.Glu184Asp
PSEN1	chr14:g.73659407A>T	c.604A>T	p.Ile202Phe
PSEN1	chr14:g.73659420G>C	c.617G>C	p.Gly206Ala
PSEN1	chr14:g.73659429G>A	c.626G>A	p.Gly209Glu
PSEN1	chr14:g.73659429G>T	c.626G>T	p.Gly209Val
PSEN1	chr14:g.73659438C>A	c.635C>A	p.Ser212Tyr
PSEN1	chr14:g.73659452G>C	c.649G>C	p.Gly217Arg
PSEN1	chr14:g.73659459T>C	c.656T>C	p.Leu219Pro
PSEN1	chr14:g.73659469G>T	c.666G>T	p.Gln222His
PSEN1	chr14:g.73659480T>G	c.677T>G	p.Leu226Arg
PSEN1	chr14:g.73659488A>T	c.685A>T	p.Ile229Phe
PSEN1	chr14:g.73659492G>A	c.689G>A	p.Ser230Asn
PSEN1	chr14:g.73659500A>C	c.697A>C	p.Met233Leu
PSEN1	chr14:g.73659501T>C	c.698T>C	p.Met233Thr
PSEN1	chr14:g.73659506C>G	c.703C>G	p.Leu235Val
PSEN1	chr14:g.73659517C>G	c.714C>G	p.Ile238Met
PSEN1	chr14:g.73659536A>C	c.733A>C	p.Thr245Pro
PSEN1	chr14:g.73664748C>G	c.779C>G	p.Ala260Gly
PSEN1	chr14:g.73664748C>T	c.779C>T	p.Ala260Val
PSEN1	chr14:g.73664750G>T	c.781G>T	p.Val261Phe
PSEN1	chr14:g.73664760C>T	c.791C>T	p.Pro264Leu
PSEN1	chr14:g.73664769C>T	c.800C>T	p.Pro267Leu
PSEN1	chr14:g.73664775G>A	c.806G>A	p.Arg269His
PSEN1	chr14:g.73664780C>G	c.811C>G	p.Leu271Val
PSEN1	chr14:g.73664793C>T	c.824C>T	p.Ala275Val
PSEN1	chr14:g.73664808A>C	c.839A>C	p.Glu280Ala
PSEN1	chr14:g.73664808A>G	c.839A>G	p.Glu280Gly
PSEN1	chr14:g.73664816T>C	c.847T>C	p.Phe283Leu
PSEN1	chr14:g.73664831T>C	c.862T>C	p.Tyr288His
PSEN1	chr14:g.73671096_73676953del5858	c.869-1998_956-1524del5858	p.S290C;T291_S319del
PSEN1	chr14:g.73673093G>A	c.869-1G>A	p.S290C;T291_S319del
PSEN1	chr14:g.73673093G>T	c.869-1G>T	p.S290C;T291_S319del
PSEN2	chr1:g.227073304A>T	c.422A>T	p.Asn141Ile

Supplemental Table 3: Effect of Reference Region on PiB PET Findings		
Reference Region:	**Domain-Based Grouping**	**Codon-Based Grouping**
Cerebellar Gray	F(9,170.96) = 5.82, p = 3.32e-7	F(1,154.99) = 21.70, p = 2.24e-6
Brainstem	F(9,173.90) = 4.85, p = 3.13e-6	F(1,156.60) = 9.70, p = 0.0036
White Matter	F(9,173.35) = 5.14, p = 1.69e-5	F(1,154.96) = 11.55, p = 0.0016

P-values shown are FDR corrected

Supplemental Table 4: Sensitivity Analyses Examining Variant Grouping x EYO Associations with Cortical PiB PET SUVR

	Effect of Domain Grouping		*Effect of Codon Grouping*	
	F Value	*p*	*F Value*	*p*
Including All Families and Groupings	F(9, 170.96) = 5.17	p = 3.13e-06	F(1, 154.99) = 21.71	p = 2.24e-05
Excluding Families with Cooks D > 1 SD from mean	F(9, 149.24) = 5.98	p = 3.14e-06	F(1, 145.15) = 24.18	p = 1.22e-05
Excluding *PSEN2* Carriers	F(8, 165.47) = 5.27	p = 2.24e-05	NA	NA
Excluding *APP* Carriers	F(8, 149.28) = 6.32	p = 3.13e-06	NA	NA
Excluding All *APOE* ε4 carriers	F(9, 107.80) = 4.81	p = 5.21e-05	F(1, 104.762) = 15.32	p = 3.23e-04
Excluding All *APOE* ε2 carriers	F(9, 139.53) = 3.18	p = 2.67e-03	F(1, 134.542) = 16.94	p = 1.51e-04
Covarying Weighted Polygenic AD Risk Scores (PRS)	F(9, 164.55) = 5.14	p = 1.70e-05	F(1, 153.69) = 21.13	p = 2.44e-05
Excluding PRS > 1 SD from mean	F(9, 139.61) = 5.68	p = 6.36e-06	F(1, 135.43) = 15.71	p = 2.58e-04

P-values shown are FDR corrected

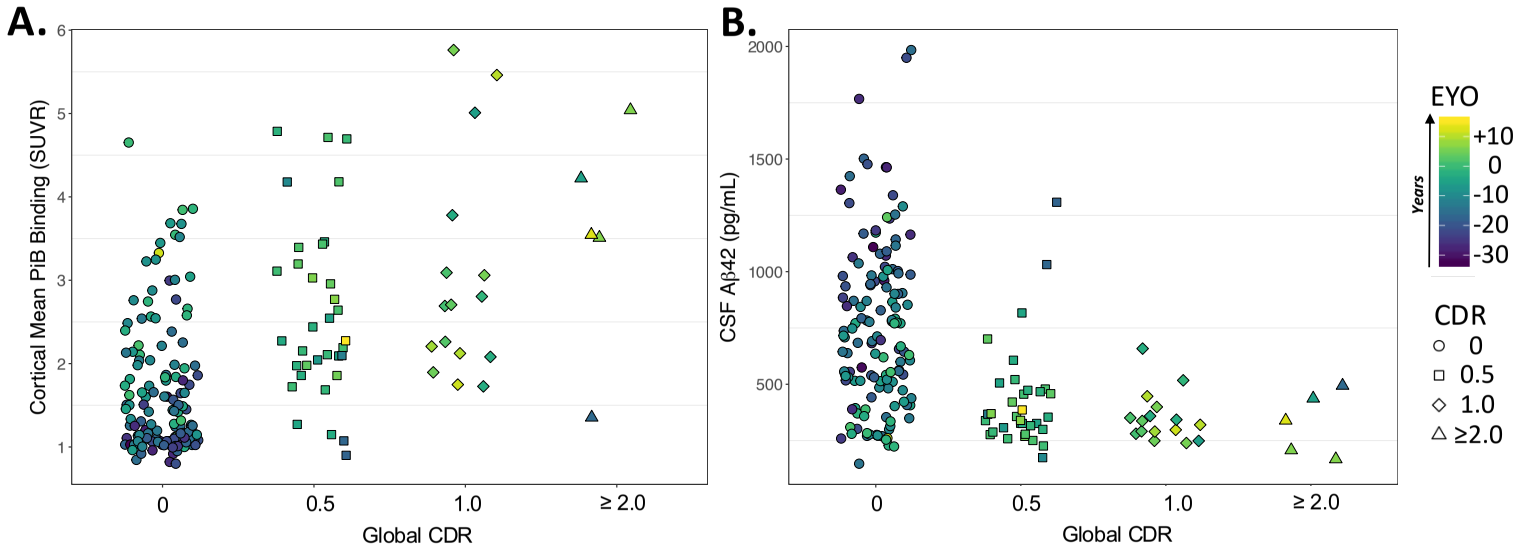

Supplemental Figure 1: *Amyloid Measures Grouped by Global Clinical Dementia Rating:* Cortical mean PiB PET binding (Panel A) and CSF Aβ42 (Panel B) in autosomal dominant Alzheimer's disease pathogenic variant carriers grouped by global Clinical Dementia Rating (CDR). Color indicates each individual pathogenic variant carrier's estimated years from symptom onset (EYO).

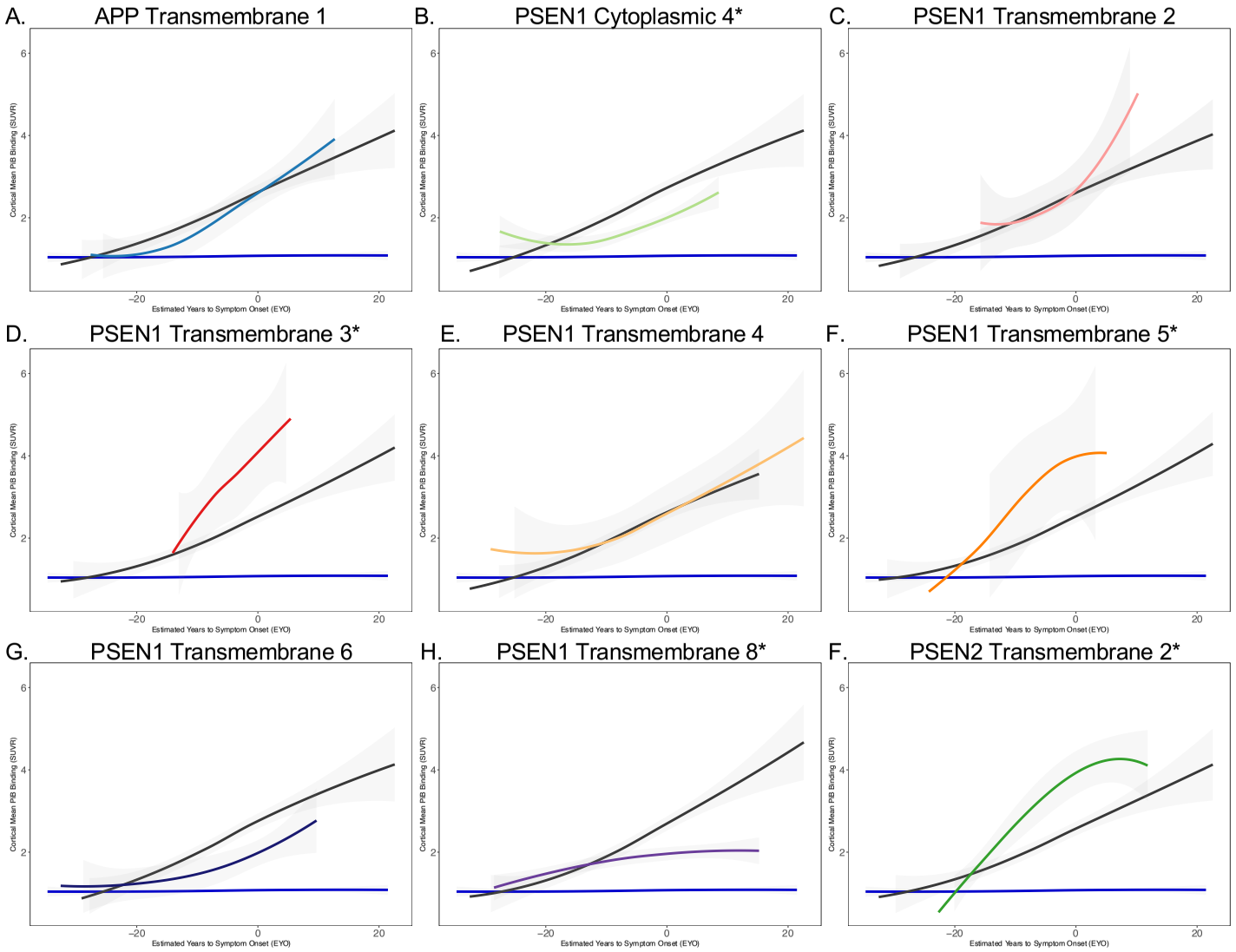

Supplemental Figure 2: *Amyloid Trajectories Differ Across Domain-based Variant Groups*: Cortical mean PiB PET binding across EYO is compared between each domain-based group (colored lines in A-F) and all other pathogenic variant carriers (Black lines). Pathogenic variant non-carriers (Blue line) are shown for illustration purposes and non-carriers were not included in statistical comparisons. * denotes FDR corrected p≤ 0.05 for a significant group by EYO interaction comparing each domain-based group to all other pathogenic variant carriers.

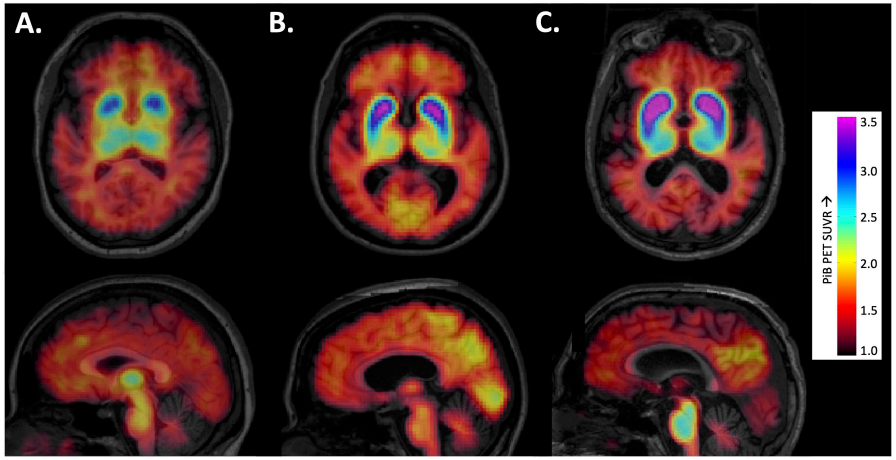

A.	B.	C.
EYO: -25 to -20	**EYO**: -5 to 0	**EYO**: 0 to +5
CDR: 0.0	**CDR**: 0.5	**CDR**: 1.0
CDR SOB: 0.0	**CDR SOB**: 3.0	**CDR SOB**: 5.5
CSF Aβ42 (pg/mL): 550	**CSF Aβ42** (pg/mL): 300	**CSF Aβ42** (pg/mL): 249
PiB Cortical Mean: 1.86	**PiB Cortical Mean:**1.98	**PiB Cortical Mean:** 1.90
PiB Striatal Mean: 3.11	**PiB Striatal Mean**: 3.73	**PiB Striatal Mean**: 4.19
Group: PSEN1 TM6	**Group:** PSEN1 TM8	**Group:** PSEN1 TM2
***PSEN1* Codon:** >200	***PSEN1* Codon:** >200	***PSEN1* Codon:** <200

Supplemental Figure 3: *Regional Variability in Amyloid Burden: Examples of Striatal Predominant Patterns.* Three examples across a range of estimated years to symptom onset (EYO) and impairment (Clinical Dementia Rating: CDR; Sum of Boxes: SOB) that show greater striatal compared to cortical amyloid burden as assessed by PiB PET. These images were chosen to demonstrate the heterogeneity present in β-amyloid measures across the course of autosomal dominant Alzheimer's disease. Transmembrane domain abbreviated as TM.

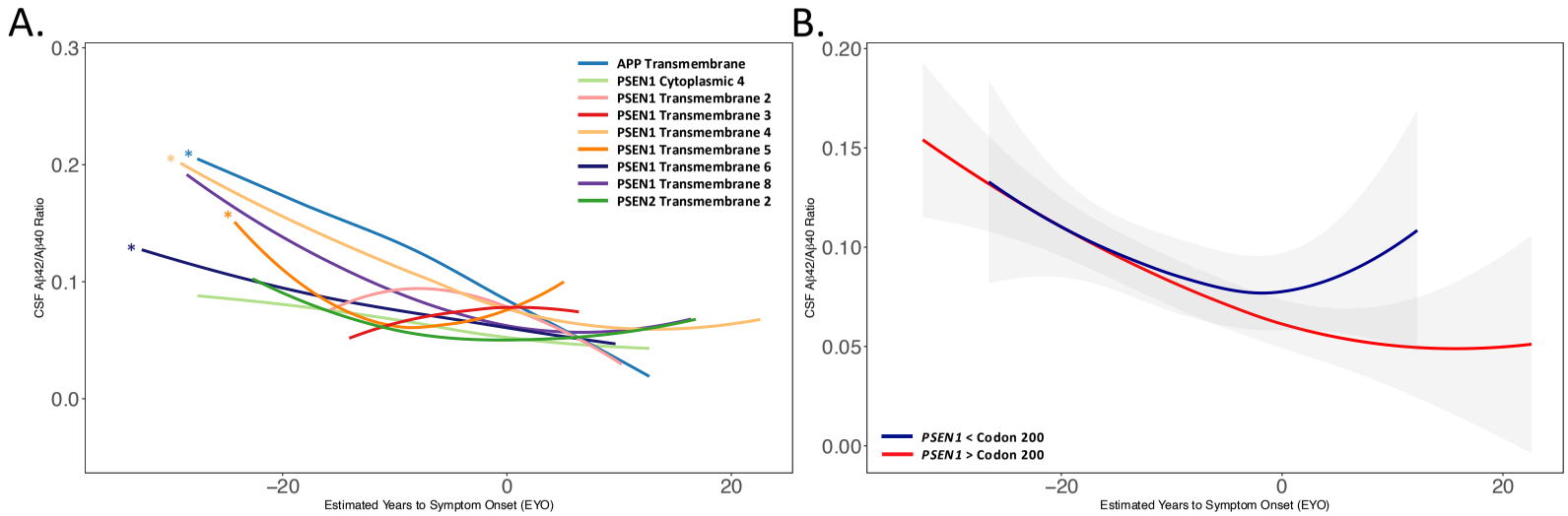

Supplemental Figure 4: *CSF Aβ42/Aβ40 across variant groupings*: Ratios of CSF Aβ42/40 were calculated for domain-based variant groupings (Panel A) and the PSEN1 codon 200 based grouping (Panel B). * denotes FDR corrected $p < 0.05$ for a significant variant group by EYO interaction.

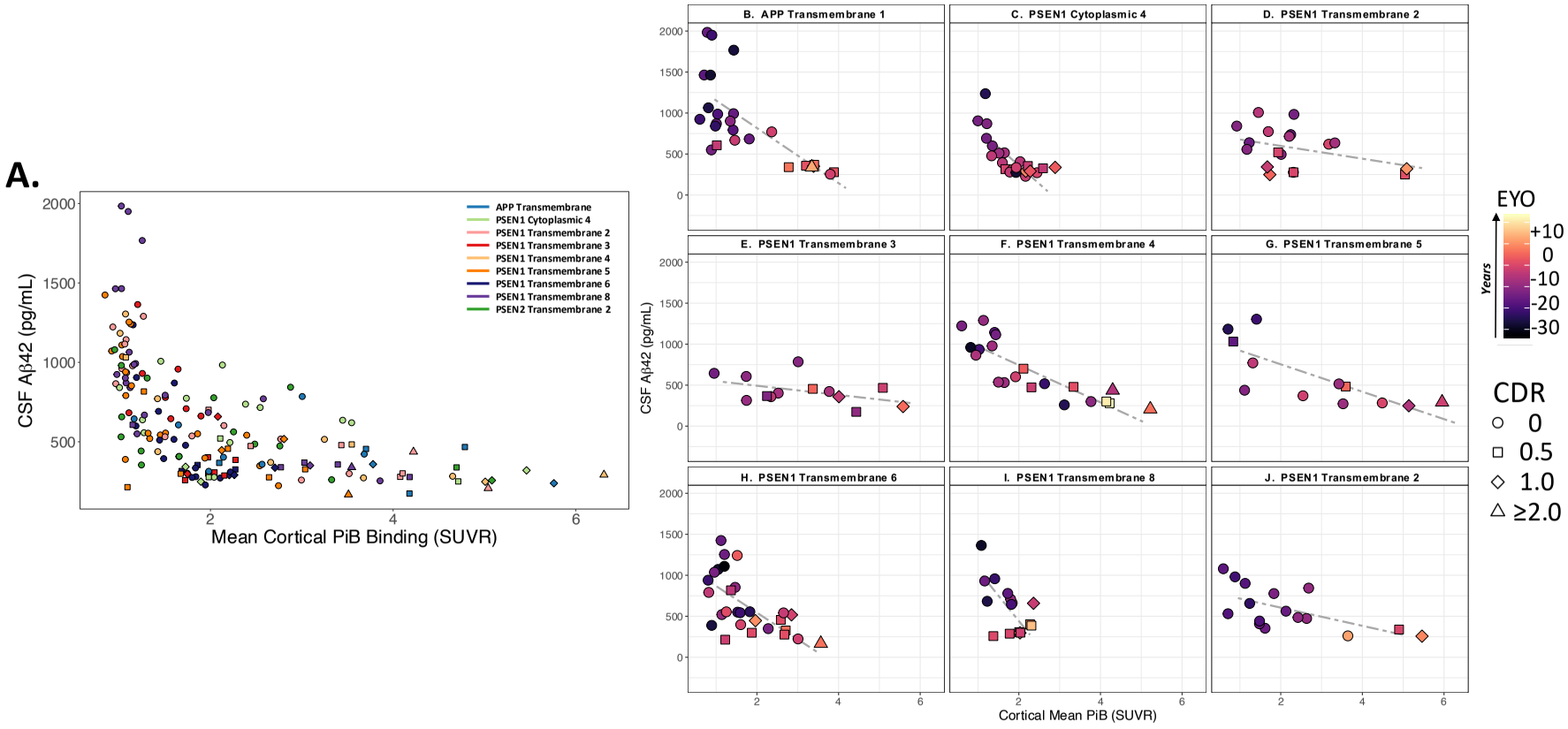

Supplemental Figure 5: *CSF Aβ42 Relative to Amyloid PET, Accounting for Variant Category:* Relationships between CSF Aβ42 and PET based measures of β-amyloid burden were assessed across all domain-based variant groupings (Panel A) and across individual variant groupings (Panels B-J). Only pathogenic variant carriers are shown.

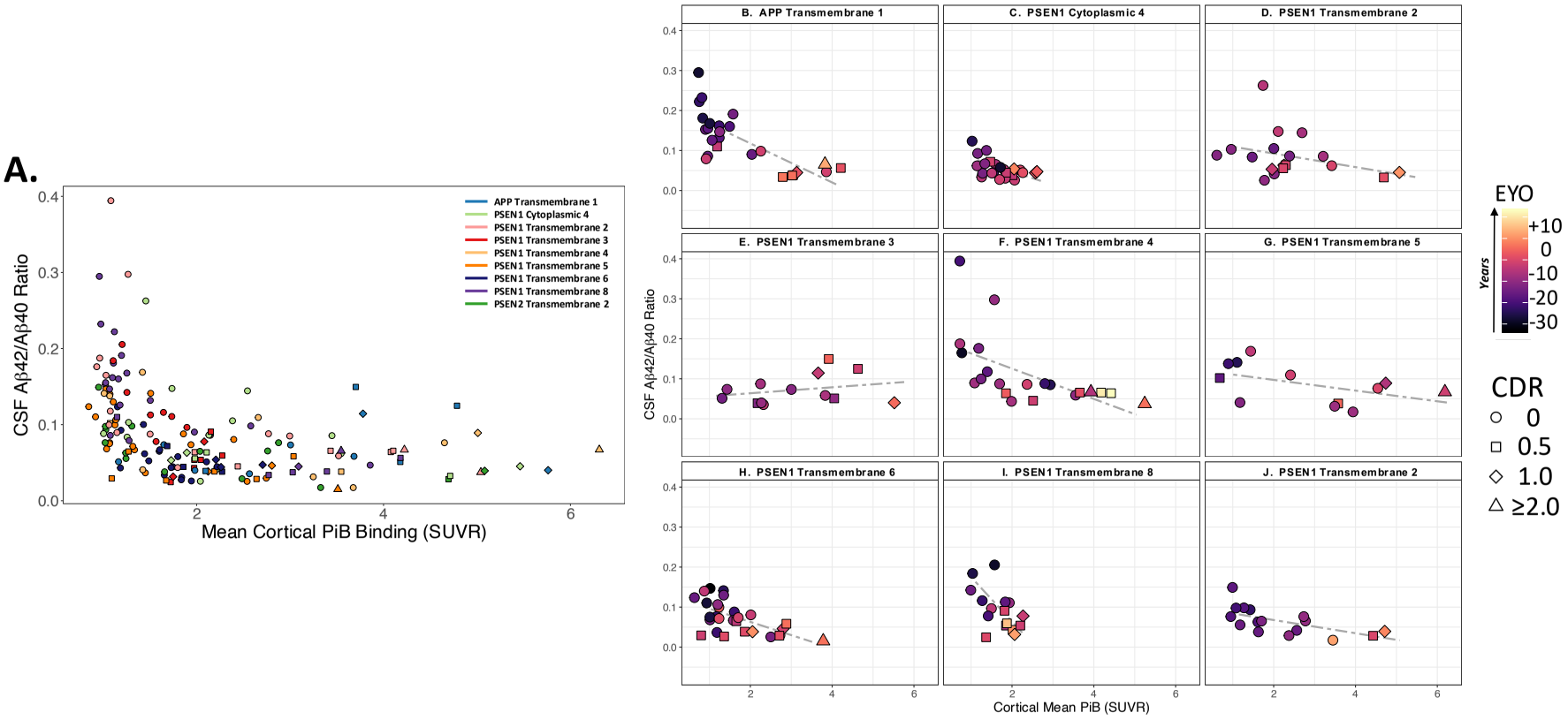

Supplemental Figure 6: *CSF Aβ42/ Aβ40 Ratio Relative to Amyloid PET, Accounting for Variant Category:* Relationships between the CSF Aβ42/40 ratio and PET based measures of β-amyloid burden were assessed across all domain-based variant groupings (Panel A) and across individual variant groupings (Panels B-J). Only pathogenic variant carriers are shown.

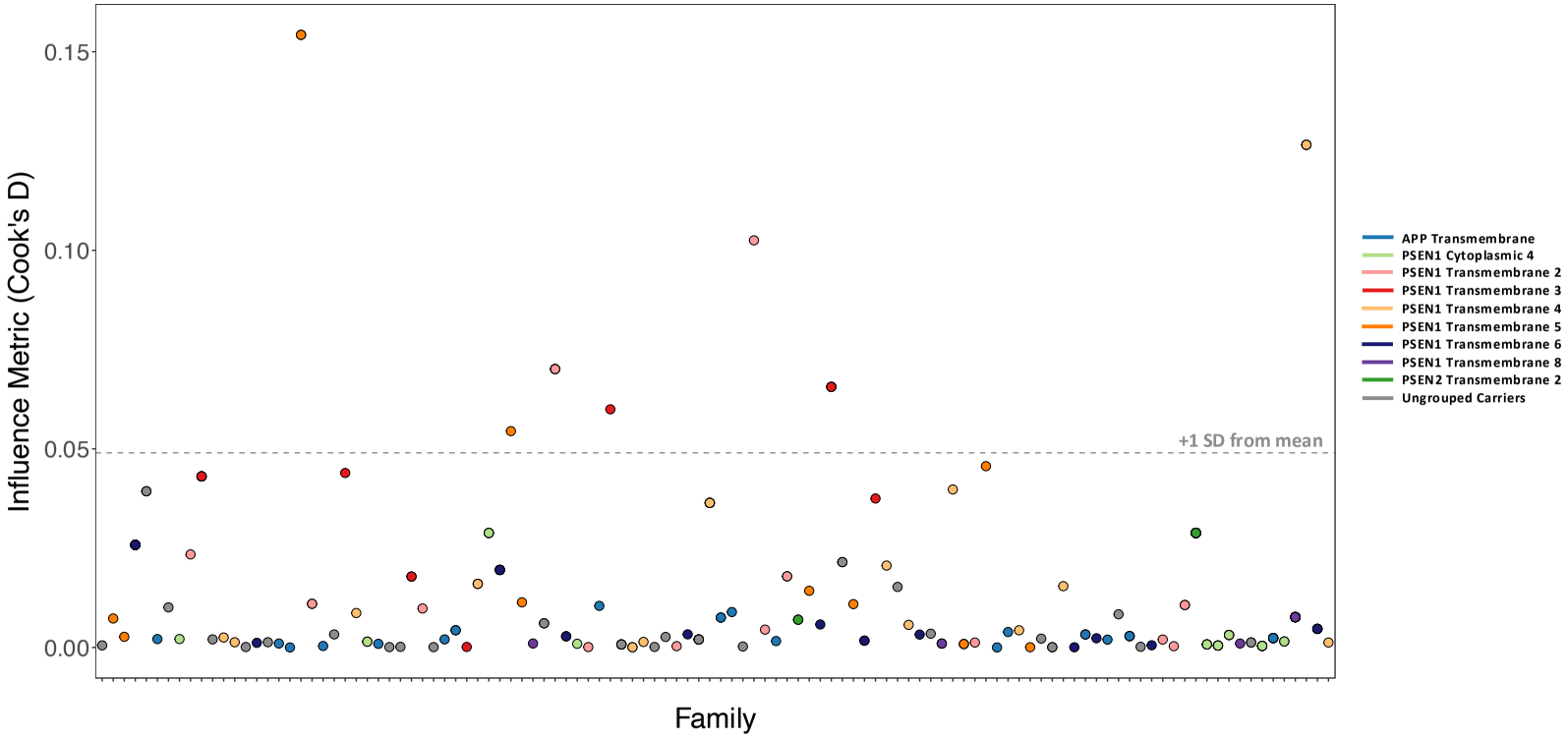

Supplemental Figure 7: *Effects of Family Membership on Amyloid PET Results:* Influence metrics were calculated for each family in the sample in models examining associations between PiB PET and domain-based variant groupings. Colors denote each domain-based group. Dashed line indicates 1 standard deviation above the group mean value for the influence metric used (Cook's D).